

*Transmitted with letter
dd 7/13/98*

**INITIAL ASSESSMENT OF DILUTION EFFECTS
INDUCED BY WATER WELL PUMPING IN THE
AMARGOSA FARMS AREA**

Prepared for

**Nuclear Regulatory Commission
Contract NRC-02-97-009**

Prepared by

**R.W. Fedors
G.W. Wittmeyer**

**Center for Nuclear Waste Regulatory Analyses
San Antonio, Texas**

**Revised
January 1998**

9809080219 980713
PDR WASTE
WM-11 PDR

ABSTRACT

A preliminary study was undertaken to gain insights into the factors controlling borehole dilution effects in the Amargosa Farms area from a potential release at the proposed Yucca Mountain repository. Dilution in individual boreholes depends on the fractions of water drawn from contaminated and uncontaminated production zones, which in turn depend on the depth of the well, screened intervals, aquifer hydraulic parameters, pumping rates, and distribution of radionuclides across a plume. Dilution arising from infiltration or groundwater mixing underneath the repository was not included in this analysis.

The fundamental question addressed by this study includes how variations in well construction practices, hydraulic parameters of the basin-fill aquifer, and pumping rates affect capture of radionuclide plumes of specified shapes. Detailed statistical analysis of magnitude and spatial distributions of water usage and well bore construction practices was conducted for the Amargosa Farms area. A sensitivity analysis for borehole dilution was performed to assess the effects of reasonable variations in aquifer hydraulic parameters, well depths, screening practices, and variations in pumping rates of irrigation and domestic supply wells for various radionuclide plume configurations. A distinction is made between dilution factors based on volumetric fluxes of the capture and plume areas and those based on dispersion during transport. In general, the volumetric flux-based dilution due to wellbore mixing reduced radionuclide concentrations by less than an order of magnitude. The range of dilution was primarily affected by pumping rates and plume thickness. The choice of modeling the plume with significant vertical dispersion (thick plume) versus little or no vertical dispersion (thin plume) had a significant impact on the borehole dilution factors. The dispersion (transport)-based dilution factors ranged from one to two orders of magnitude with the conservative lower bound delineated by the ratio of the source concentration and the centerline concentration of a plume.

CONTENTS

Section	Page
1 INTRODUCTION	1-1
1.1 GEOSPHERE RELEASE PATHWAYS CONSIDERED IN TSPA	1-4
1.2 LITERATURE REVIEW	1-4
1.3 METHODS USED TO CONDUCT STUDY	1-5
1.4 LIMITATIONS OF STUDY	1-6
2 HYDROGEOLOGY OF THE AMARGOSA DESERT	2-1
2.1 STRUCTURE AND DEPOSITIONAL HISTORY	2-1
2.2 BASIN-SCALE GROUNDWATER FLOW	2-2
3 WELL CONSTRUCTION AND WATER USE IN THE AMARGOSA FARMS AREA . . .	3-1
3.1 NUMBER AND DISTRIBUTION OF WELLS	3-1
3.2 STATISTICAL ANALYSIS OF WELL CONSTRUCTION PRACTICES	3-2
3.3 ESTIMATION OF WATER USE	3-2
4 THREE-DIMENSIONAL CAPTURE ZONE ANALYSIS AND PLUME DELINEATION .	4-1
4.1 DETERMINATION OF FLOW FIELD AND CAPTURE ZONE	4-3
4.1.1 Description of the Analytic Element Method	4-3
4.1.2 Ranges for Parameter Values	4-3
4.1.3 Sensitivity Analysis for Capture Zone	4-4
4.2 RADIONUCLIDE PLUME SHAPE AND LOCATION	4-8
4.2.1 Transport Parameters	4-10
4.2.2 Plume Dimensions for 3D Dispersion from Constant Concentration Source	4-11
4.2.3 Plume Dimensions Neglecting Vertical Dispersion for Constant Concentration Source	4-12
4.3 BOREHOLE DILUTION FACTORS BASED ON VOLUMETRIC FLUX	4-13
4.3.1 Domestic Wells	4-14
4.3.2 Irrigation Wells and Plumes with No Vertical Dispersion	4-19
4.3.3 Irrigation Wells and Plume with Vertical Dispersion	4-19
4.4 BOREHOLE DILUTION FACTORS BASED ON DISPERSIVE TRANSPORT	4-24
4.4.1 Domestic Wells	4-24
4.4.2 Irrigation Wells	4-24
5 CONCLUSIONS	5-1
6 REFERENCES	6-1
APPENDIX A — DETAILED WATER USE TABLES FOR 1983, 1985-1996	
APPENDIX B — CAPTURE ZONE DELINEATION TABLE	
APPENDIX C — TABLE OF BOREHOLE DILUTION FACTORS	

FIGURES

Figure		Page
1-1	Lower Amargosa Desert region south of proposed Yucca Mountain repository site (R) including Amargosa Valley and Amargosa Farms	1-2
3-1	The distribution of domestic and quasi-municipal wells based on range and township from well driller's logs	3-4
3-2	Distribution of annual water use (acre-ft) by type and by range and township for commercial, irrigation, quasi-municipal wells for the year 1996	3-7
3-3	Distribution of water use by type for the year 1996	3-8
4-1	Comparison of plume cross-section (P), irrigation well capture area (I), and domestic well capture area (D)	4-2
4-2	This plot illustrates the effect of well penetration depth (60, 190, 500, and 1,000 m) on a small irrigation capture zone width and thickness	4-5
4-3	Effect of combinations of transmissivity (200, 300, 400 m ² /d) and hydraulic head gradient (0.001, 0.002, 0.003, 0.005) on a large irrigation well's capture zone width and thickness	4-6
4-4	Effect of combinations of transmissivity (50, 100, 200, 300, 400 m ² /d) and hydraulic head gradient (0.001, 0.0025, 0.005, 0.01) on a domestic well's capture zone width and thickness	4-7
4-5	This plot illustrates the effect of pump rate (range 1 to 2000 m ³ /d) on the capture zone width and thickness	4-9
4-6	Effect of pump rate (range 1 to 75 m ³ /d) on the flux-based borehole dilution factor for plumes of thickness 10 m and 25 m (no vertical dispersion)	4-15
4-7	Effect of screen position for domestic-sized wells on the flux-based borehole dilution factor for plumes of thickness 10 m and 25 m (no vertical dispersion)	4-16
4-8	Effect of transmissivity (10, 50, 100, 400 m ² /d) on the flux-based borehole dilution factor for plumes of thickness 10 m and 25 m (no vertical dispersion)	4-17
4-9	Effect of the regional gradient (0.001, 0.0025, 0.005, 0.01) on the flux-based borehole dilution factor for a domestic-sized well and plumes of thickness 10 m and 25 m (no vertical dispersion)	4-18
4-10	Effect of pump rate on flux-based borehole dilution factors for irrigation wells and a 25 m thick plume with no vertical dispersion	4-20
4-11	Effect of pump rate on dilution factors for irrigation sized wells and a plume with 3D dispersion	4-21
4-12	Effect of transmissivity (50 to 400 m ² /d) on dilution factors for irrigation sized wells and a plume with 3D dispersion	4-22
4-13	Effect of regional hydraulic gradient (0.001 to 0.0005) on dilution factors for irrigation-sized wells and a plume with 3D dispersion	4-23
4-14	Effect of pumping rate (1-75 m ³ /d) for domestic wells on transport dispersion-based borehole dilution factor for two different plume configurations: a thin plume with no vertical dispersion and a 3D dispersion plume both with dispersivity ratios as noted in the plot	4-25

FIGURES (Cont'd)

Figure		Page
4-15	Effect of transmissivity (10–400 m ² /d) for domestic wells (Q = 3 m ³ /d) on transport dispersion-based borehole dilution factor for two different plume configurations: a thin plume with no vertical dispersion and a 3D dispersion plume, both with dispersivity ratios as noted in the plot	4-26
4-16	Effect of pumping rate (300–2,000 m ³ /d) for irrigation wells on transport dispersion-based borehole dilution factor for four different plume configurations: two thin plumes with no vertical dispersion and two 3D dispersion plumes, all with dispersivity ratios as noted in the plot	4-27
4-17	Effect of transmissivity (50–400 m ² /d) for large irrigation wells (Q = 2116 m ³ /d) on transport dispersion-based borehole dilution factor for two different plume configurations: two 3D dispersion plumes with dispersivity ratios as noted in the plot	4-28

TABLES

Table	Page
3-1 Distribution of wells by water use across Townships T15,16,17S using well driller's logs .	3-3
3-2 Statistics for well construction practices and water level positions for wells recorded in GWSI database in Amargosa Valley and Amargosa Farms area	3-3
3-3 Annual estimates of water use by type; International Minerals Venture Floridan (IMV), American Borate (AB), quasi-municipal (QM), commercial (COM)	3-5
3-4 Summary statistics of individual irrigation users on an annual basis	3-6
4-1 Plume configuration and point dilution factor at 15 km from the source area for a range of dispersivity values. C_c is the centerline concentration. The source area is 25 m thick by 500 m wide.	4-13
4-2 Plume configuration and point dilution factor at 25 km from source area for a range of dispersivity values	4-13
4-3 Plume configuration in terms of width at 15 and 25 km and point dilution factor for a source area width of 500 m and no vertical dispersion	4-14

ACKNOWLEDGMENTS

This report was prepared to document work performed by the Center for Nuclear Waste Regulatory Analyses (CNWRA) for the Nuclear Regulatory Commission (NRC) under Contract No. NRC-02-97-009. The activities reported here were performed on behalf of the NRC Office of Nuclear Material Safety and Safeguards (NMSS), Division of Waste Management (DWM). The authors thank Chad Glenn (NRC) for his assistance in obtaining data from the Nevada Division of Waster Resources, Ron Martin for his assistance with geographic information (GIS) data; J. Winterle, A. Armstrong, and R. Baca for their technical reviews; and B. Sagar for his programmatic review. The authors would also like to thank C. Gray for his editorial review and C. Garcia for secretarial support. The report is an independent product of the CNWRA and does not necessarily reflect the views or regulatory position of the NRC.

QUALITY OF DATA, ANALYSES, AND CODE DEVELOPMENT

DATA: CNWRA-generated original data contained in this report meet quality assurance requirements described in the CNWRA Quality Assurance Manual. Sources for other data should be consulted for determining the level of quality for those data.

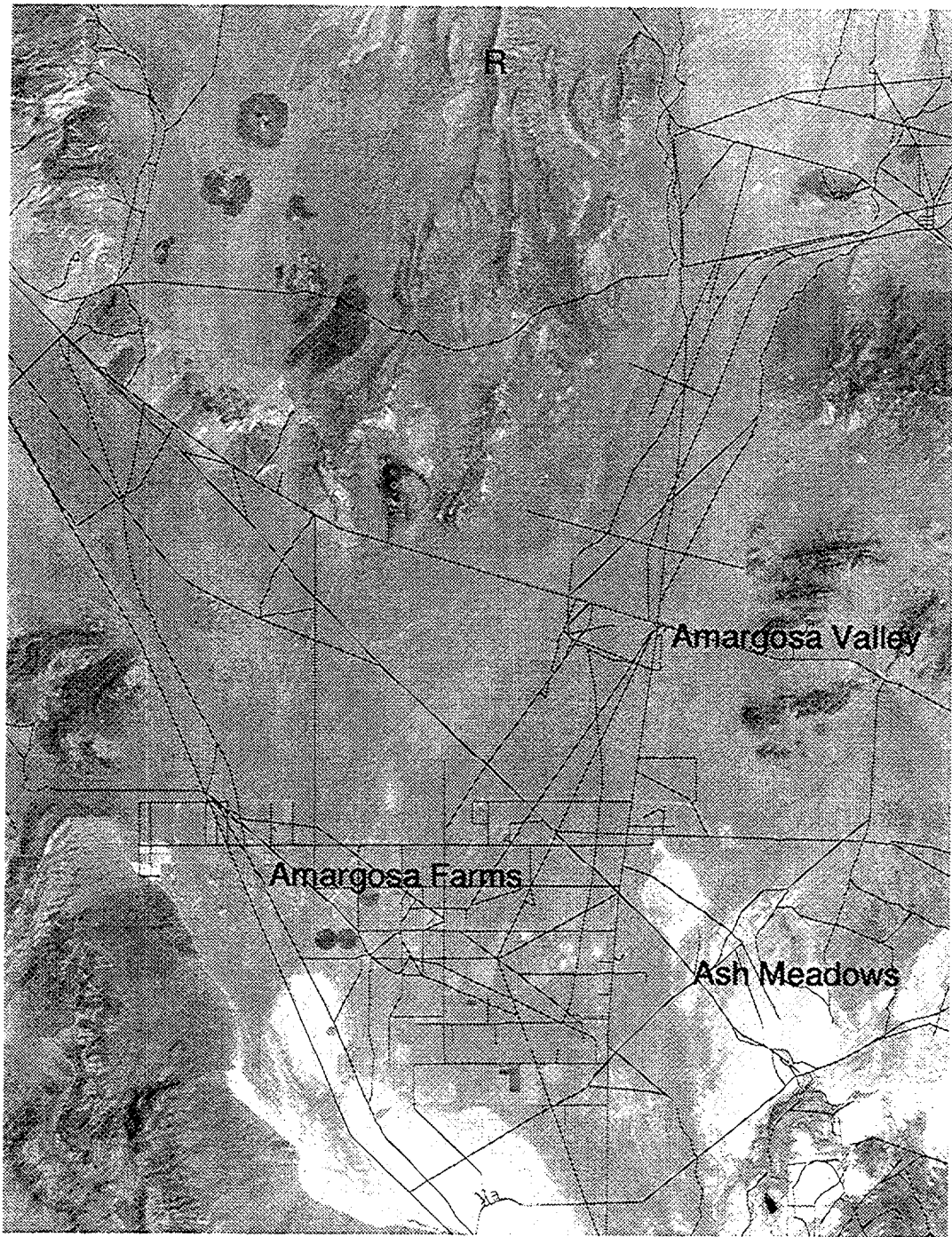
ANALYSES AND CODES: The GFLOW Version 1.1, PATCHI Version 1.1, and STRIPI Version 1.1 computer codes were used for analyses contained in this report. These computer codes are controlled under the CNWRA Software Configuration Procedures.

1 INTRODUCTION

Yucca Mountain (YM), Nevada, was originally proposed as a deep geologic repository for high-level radioactive waste due in part to its favorable hydrogeologic regime. Moisture fluxes within the 700 m thick unsaturated zone at YM were presumed to be small (< 0.1 mm/yr) due to the region's arid climate and the low permeability of the tuff units comprising the mountain (U.S. Department of Energy, 1988). Low moisture fluxes should reduce the rate of waste canister corrosion, subsequent dissolution of the exposed waste form, and transport of radionuclides to the accessible environments. However, recent studies (Stothoff, 1997; Flint and Flint, 1994) suggest that mean annual infiltration at YM may be as high as 15 mm and provide convincing evidence that there are fast pathways, albeit probably spatially focused, from the surface of YM to at least the depth of the repository (Fabryka-Martin et al., 1996). Radionuclides not sorbed by the zeolitized bedded tuffs that underlie the repository (e.g., technetium, iodine, neptunium), or diffused from fluid-conducting fractures into the rock matrix within welded tuff units, will enter the water table, which, based on current engineering designs, lies 250 to 300 m below the repository. Current hydrogeologic studies (Czarnecki and Waddell, 1984; TRW Environmental Safety Systems, Inc., 1995) indicate that radionuclides that enter the saturated zone beneath YM would generally flow to the south-southeast into western Jackass Flat within the welded tuff aquifer and then south-southwest into the Amargosa Desert where the water table lies within an alluvial aquifer. In order to demonstrate compliance with a risk- or dose-based standard, mixing that occurs due to saturated zone transport and active pumping of wells may play a major role in reducing radionuclide concentrations.

Saturated zone dilution of radionuclide concentrations depends on the bulk flow rate of water beneath YM at locations where radionuclides enter the water table, the degree of mixing caused by large-scale variations in the groundwater velocity field in the welded tuff and alluvial aquifers, and mixing in boreholes where water may be pumped for domestic or agricultural use. Clearly, the amount of dilution depends on the duration and degree of mixing along the radionuclide transport path, while the estimated risk or dose depends on the ultimate use of water pumped from the aquifer. Estimating dose or risk requires definition of a potentially exposed population and the potential biosphere pathway by which an individual would be exposed to released radionuclides (TRW Environmental Safety Systems, Inc., 1995). In the TSPA-95 (TRW Environmental Safety Systems, Inc., 1995), it was assumed that the peak dose to the maximally exposed individual is received by a person drinking 2 L of water per day pumped from the welded tuff aquifer at a location just outside the boundary of the controlled area (5 km outside the repository footprint). However, National Academy of Sciences recommendations may require determining the peak dose to the average member of a critical group, based on current water and land use practices in the YM area. Therefore, it is prudent to consider populations currently residing downgradient from YM, such as the Amargosa Farms area (figure 1-1), that produce at least a portion of the food they consume using local groundwater to irrigate their crops. However, one should consider variations in individual expected dose within the critical group due to differences in well locations, well construction, and pumping rates.

As noted in Kessler and McGuire (1996), dispersive transport processes are relatively ineffective at reducing contaminant concentrations in a steady-state groundwater flow regime. If there are large temporal variations in the magnitude and direction of the groundwater velocity field, then mixing and attendant dilution during transport may be significant. Current conceptual models of the YM saturated groundwater system would suggest that the flow regime is relatively unperturbed by fluctuations in the magnitude and location of recharge and discharge. However, increased pumping for irrigated agriculture in the Amargosa Farms area over the past 30 yr may have had some effect on the groundwater flow



Scale 1:250000

Figure 1-1. Lower Amargosa Desert region south of proposed Yucca Mountain repository site (R) including Amargosa Valley and Amargosa Farms

regime. Nonetheless, in the present study it is assumed that pumping has no effect on the groundwater flow regime between YM and receptor locations. If the primary effect of pumping on the flow regime is enhanced mixing or more rapid transport, the assumption of steady state flow conditions, if not realistic, is at least conservative from the standpoint of radionuclide dose.

Dilution factors can be defined in a number of ways. Each of the three definitions mentioned in this report are based on a particular approach to addressing dilution. The first approach addresses dilution that results from dispersion of a solute during transport; the dilution factor is calculated as the ratio of concentration at the source area to that at the receptor point. The second approach addresses dilution due to mixing and is calculated as the mass release rate divided by the largest flux of water into which the solute may be mixed and used by a critical group. The third approach addresses dilution due to the intersection of the capture zone of a pumping well with the plume configuration at the withdrawal location. In this case, the dilution factor is calculated as the ratio of the plume area intercepted by the capture area and the entire capture area. The third approach is used in this report to describe borehole dilution from the geometric standpoint and it may be linearly combined with the first approach for a total borehole dilution factor. Usage of the first two approaches is described further below.

Baca et al. (1997) and Kessler and McGuire (1996) used the first approach to calculate point dilution factors (P-DF) where point refers to concentration at a single point. Under assumptions of steady state flow, estimated dilution factors due to dispersive mixing along the saturated zone transport pathway from the proposed YM repository to locations 20 to 30 km to the south have ranged from 5 to 50 (Baca et al., 1997) and from 4 to 44 (Kessler and McGuire, 1996). In both analyses, the reported dilution factors were determined by solving the advection-dispersion equation. Baca et al. (1997) contoured the P-DF while Kessler and McGuire (1996) tabulated P-DFs based on centerline concentration. In TSPA-93 (Wilson et al., 1994), TSPA-95 (TRW Environmental Safety Systems, Inc., 1995), and Iterative Performance Assessment Phase 2 (Nuclear Regulatory Commission, 1995) it was assumed that additional dilution occurs at the receptor location due to mixing of clean and contaminated water in the borehole and, in the case of TSPA-95, due to mixing of waters from groundwater basins influent to the central region of the Amargosa Desert.

In the ongoing NRC Iterative Performance Assessment (IPA) Phase 3, the borehole dilution factor corresponds to a single well that is pumped at a rate sufficient to supply all water needs for the critical group in question. For example, if there are assumed to be 12 quarter-section, center pivot irrigation plots under cultivation with alfalfa at Amargosa Farms, the equivalent annual well discharge¹ is 9,300,000 m³. If the critical group consists of a residential community of 500 persons located 5 km south of YM, the equivalent annual well discharge² would be 103,700 m³. Borehole dilution factors can be computed directly for the critical groups if the volume of contaminated water captured by the well is known. For example, if, the volume of contaminated water captured by the well at Amargosa Farms is 930,000 m³, the dilution factor is 10. However, in order to determine a dose, one must compute the radionuclide concentration in the borehole and, hence must also know the concentration of radionuclides in the contaminated water captured by the well. Inherent in this approach, the assumption is that the entire radionuclide plume is captured and that there is no well-to-well variation in the concentration. This report

¹ 12 plots × 126 acres/plot × 5 ft of water/year ÷ (8.107 × 10⁻⁴ m³/acre-ft).

² 150 gal/person-day × 500 persons × 365.25 days/yr × 3.785 × 10⁻³ m³/gal.

addresses the validity of this assumption considering the concept of borehole dilution as well as the distribution of pumping well locations and pump magnitudes.

1.1 GEOSPHERE RELEASE PATHWAYS CONSIDERED IN TSPA

Farming in the Amargosa Farms region is partially related to the accessibility to well water. The combination of non-arable land and large depths to the water table restrict farming-based population growth to the area immediately south of the town of Amargosa Valley. The water table gradually approaches the land surface toward the southern reaches of the Amargosa Farms area. Exposure scenarios are assumed to occur through a combination of drinking water and ingestion of locally raised produce and livestock. The lengths of the groundwater flow paths from YM to domestic and commercial wells and irrigation wells are approximately 25 and 30 km, respectively.

1.2 LITERATURE REVIEW

In groundwater hydrology, the term borehole dilution is used to describe several phenomena including: (i) contaminant sampling biases resulting from improper monitor well construction, (ii) the effectiveness of pump and treat remediation systems, and (iii) capture zone analysis. Borehole dilution is used to explain one to two order-of-magnitude differences in values between concentrations measured in sampling wells and concentrations measured in the aquifer; however, the concentration in the borehole may be greater than the *in situ* or resident concentration. Borehole dilution is also the name of a procedure used to estimate permeabilities or seepage velocity in a single well bore through analysis of the dilution rate after release of a solute in the wellbore. Borehole dilution in the present work refers to dilution of the resident contaminant concentrations in a wellbore due to pumping a well that captures both contaminated and uncontaminated portions of the aquifer.

Six factors that may significantly affect the borehole concentration are: (i) well pump rate and well distribution in the well field, (ii) regional hydraulic gradient, (iii) transmissivity, (iv) hydrostratigraphy and anisotropy, (v) well penetration depth and length of screen, and (vi) vertical and horizontal contaminant plume distribution. Analytical solutions for flow can incorporate the effects of well pump rates, well design, and regional gradients under certain restrictions for a sensitivity analysis. Complex numerical models are generally required to analyze the effects of heterogeneity in the hydraulic properties and simulate complex plume configurations, especially if three-dimensional (3D) effects are considered to be important. An increase in the spacing of the wells may increase the capture zone horizontally but may decrease the capture zone vertically and may introduce gaps in the capture zone between wells where contaminants may escape. An increase in the regional hydraulic gradient will act to decrease the capture area. An increase in the anisotropy will increase the capture zone horizontally but decrease it vertically.

Analytic solutions (Schafer, 1996; Faybishenko, et al., 1995; Grubb, 1993) and analytic element methods (Strack, 1989; Haitjema, 1995) have been published for estimating capture zones for partially penetrating wells in steady state 3D flow fields. Sensitivity analyses of effects that include vertical movement of water or solute in a heterogeneous domain require the use of numerical models. A good illustration of the factors that affect capture zone size and shape is found in Bair and Lahm (1996). Bair and Lahm (1996) used a finite difference method to determine the steady state flow field and particle tracking to delineate the size and shape of the capture zone. They determined the magnitude of changes to the capture zone area due to perturbations in the regional gradient, well penetration, pump rates, well

configuration, and degree of hydraulic conductivity anisotropy in the context of an idealized pump and treat design.

Three published articles on numerical simulation of 3D flow in and around a wellbore contain pertinent information for refined modeling in the vicinity of a single well. Chiang et al. (1995) simulated 3D flow and advective solute transport in the vicinity of a partially penetrating well in order to understand the order of magnitude difference in contaminant concentrations between well samples and point aquifer samples. The concentration profile in the aquifer was known. The well bore was modeled as separate elements with a permeability in the range of that predicted for laminar flow in a tube. They noted that their transient simulation results asymptotically approached the simple, mass balance-based result which assumes a flat water table.

Akindunni et al. (1995) simulated 3D flow near a well for various screen and plume positions. They approximated the well using a Neumann boundary condition at the edge of the domain at which the discharge was equally apportioned to the nodes along the screened length of the well. They compared vertically averaged values of concentration for both the wellbore and the aquifer. In the transient simulations, concentrations differed significantly in the well and aquifer. Concentrations in the wellbore were higher or lower than the vertically averaged aquifer value depending on the relative position of the plume depth and screened interval. However, over long times, the concentration in the wellbore asymptotically approached the vertically averaged aquifer value. In addition to screen position and plume position, they also investigated the dependence on screen length and anisotropy. Again, initial concentrations differed significantly but long time concentrations appeared to approach the vertically averaged aquifer value. As expected, simulations with large anisotropy ratios for hydraulic conductivity exhibited less vertical mixing than the isotropic case.

Reilly et al. (1989) also modeled the wellbore as a column of hydraulically connected cells; however, their focus was on wellbore flow in a monitoring well with implications for sampling bias and cross-contamination. In a monitoring well, cross-contamination will act to dilute the plume. Of note was their conclusion that greater than half the aquifer-to-wellbore flow occurred in the top ten percent of the screened length while greater than half the wellbore-to-aquifer flow occurred in the bottom ten percent of the screened length. Hence, solute plumes approaching the top of the screened portion will enter the wellbore while plumes approaching the bottom will tend to flow around the well. This finding may be pertinent for the Amargosa Farms area when irrigation wells are shut down, but is probably irrelevant during periods of pumping.

1.3 METHODS USED TO CONDUCT STUDY

Wellbore design and pumping practices in the Amargosa Farms region may have a significant effect both on the capture of a potential plume and, from another perspective, on the radionuclide concentration of the water pumped from the wells. Existing databases were analyzed in order to characterize the location, design, and production of wells. An important feature of the wells in the Amargosa Farms region is that they partially penetrate the alluvial aquifer thickness. The first wells encountered in a path of a simulated plume released from the proposed repository site are low pumping rate domestic, commercial, and quasi-municipal wells at a distance of approximately 25 km. Large pumping rate irrigation wells capable of lowering the water table over square kilometers of area are located at a distance of approximately 30 km.

The analytic element method is used to model 3D flow in the vicinity of a partially penetrating well. Particle tracking is used to delineate a capture area for different well designs, pumping rates, and regional flow characteristics. The capture area is determined at an upgradient point from the well location where the flow is essentially one-dimensional (1D); for example, no longer 3D. Also, the cross-sectional area of a plume entering the Amargosa Farms region is approximated by using two-dimensional (2D) and 3D solutions to the advection-dispersion equation. Geometric arguments are utilized to estimate dilution factors due to the portion of the plume captured. For dilution factors based on dispersive transport, numerical integration is used to estimate a representative concentration for the portion of the plume captured.

1.4 LIMITATIONS OF STUDY

The geometric borehole dilution factors reported here account only for borehole dilution due to pumping in the Amargosa Farms area. Dilution due to mixing with clean water, either underneath the repository or at the northern portion of Fortymile Wash, or from any interbasin transfers is not included. The dilution factors calculated using the different approach may not be linearly combined nor directly compared except under certain restrictions. A comparison of the Total-system Performance Assessment (TPA) streamtubes of Baca et al. (1997) with the geometries of the capture zone and plume configuration are not possible since they are derived from different phenomena.

Three significant assumptions are used in this study, in part due to the scarce amount of data for the groundwater in the alluvial sediments of Amargosa Farms region. Material properties are considered to be homogeneous and isotropic, the flow field is assumed to be uniform, and steady state pumping rate and contaminant transport are assumed to represent the effects of borehole dilution. The latter assumption specifically addresses that the irrigation pumping patterns can be approximated by an annual pump volume. The dilution factors calculated for steady state flow and transport provide an upper bound for those that would result from a transient analysis.

This study addresses borehole dilution induced by a single well, pumping at a rate comparable to an actual well in the Amargosa Farms area. This differs from the IPA Phase 3 approach where the entire volume of water needed by the critical group is used in determining radionuclide concentrations for dose calculations, hence all the wells are assumed equally mixed.

2 HYDROGEOLOGY OF THE AMARGOSA DESERT

The Amargosa Desert is a northwest-trending, triangular-shaped alluvial basin bounded on the north by Bare Mountain, YM, and the Specter Range, on the east by the Resting Spring Range, and on the west by the Funeral Range and Black Mountains. Elevations on the valley floor range from 975 m mean sea level (msl) at the Amargosa River narrows near Beatty and 720 m (msl) at the proximal edge of the fan formed by Fortymile Wash as it discharges from Jackass Flat to less than 610 m (msl) at Franklin Lake playa south of the Amargosa Farms region.

2.1 STRUCTURE AND DEPOSITIONAL HISTORY

The Amargosa Desert is an alluvial valley that resulted from large-scale block faulting in the Basin and Range Province (Plume, 1996; Bedinger et al., 1989). Sediments deposited in depressions created by Tertiary to Quaternary block faulting can be classified as alluvial fan, lake bed, and fluvial deposits. In general, the coarsest materials (gravels and boulders) were deposited near the mountains, and the finer materials (silts and clays) were deposited in the central part of the basin. The distribution of sediment is generally associated with distance from the mountains. Alluvial fans with steep gradients and coarse sediments flatten and coalesce basinward, interfingering with the lake bed deposits. Within the alluvial fans there is a complex interfingering and interbedding of fine and coarse sediments due to shifting of fluvial processes across the top of the fan. The finer grained, distal portions of the fans merge laterally and interlayer with the lake deposits. The lake bed deposits can include beach sand and gravel lenses, silts and clay layers, and evaporites from playa-type environments. The fluvial deposits of recent times consist of sand and gravel lenses along present or ancestral streams. These exhibit a greater degree of sorting than the alluvial fan deposits.

Repeated upheaval events led to a complex interbedding and interlayering of the proximal and distal facies of the alluvial basin sediments. The repeated upheavals, together with the lateral and down gradient transitions within the alluvial fan and grading into the lake bed or playa deposits, has strong implications for flow and transport on a basin-wide scale.

The Amargosa Farms region is in the distal portion in terms of sediment facies of an alluvial basin where lowland fans and lake beds would comprise much, but not all, of the stratigraphic section. Geologic lithologies and maps are described in Burchfiel (1966), Denny and Drewes (1965), Fischer (1992), Naff (1973), Swadley (1983), Swadley and Carr (1980), and Walker and Eakin (1963). Recent maps of the central Amargosa Desert area have followed the lithologic characterization of Hoover et al. (1981). Local features pertinent to the hydrogeology include the presence of tuffaceous beds (ash fall), limestone horizons, perched water systems (especially where the Funeral Mountain fan conglomerates overlie lake sediments), common occurrence of caliche, and cementation of sand and gravel units. The high east-west hydraulic gradient, in the otherwise north-south regional gradient, between Amargosa Farms and Ash Meadows is thought to be due to low permeability lake bed sediments faulted into juxtaposition with the conductive Paleozoic carbonates of Ash Meadows.

The thickness of the alluvial sediments in the Amargosa Farms region is not well known. Bedinger et al. (1989) report the basin-fill as greater than 1,300 m, possibly as thick as 2,000 m for basins in the Death Valley Region. Oatfield and Czarnecki (1991) used geophysical data to estimate the thickness of the alluvial valley fill sediments in the range 800 to 1,100 m for the Amargosa Farms area.

Laczniak et al. (1996) infer depths up to 1,140 m on their east-west cross-section across the Amargosa Farms area.

2.2 BASIN-SCALE GROUNDWATER FLOW

Hydrographically, Amargosa Desert is part of the Death Valley groundwater flow system, which is a series of topographically closed intermontane basins connected at depth by the Paleozoic carbonate aquifer. The Death Valley groundwater system is further subdivided into three basins: (i) the Alkali Flat-Furnace Creek Ranch sub-basin; (ii) the Ash Meadows sub-basin; and (iii) the Oasis Valley sub-basin. The Amargosa Farms region is in the southern portion of the Alkali Flat-Furnace Creek sub-basin and adjacent to the Ash Meadows sub-basin (D'Agnese et al., 1996; U.S. Department of Energy, 1988). The Ash Meadows sub-basin, which drains the eastern and northeastern basins of the Death Valley regional flow system, is not believed to be influent to Alkali Flat-Furnace Creek Ranch sub-basin in the vicinity of the primary agricultural pumping area.

The diverse mix of geochemical signatures in the Amargosa Desert area suggests that the groundwater comes from a combination interbasin flow, upwelling from the deep Paleozoic carbonate aquifer, and intrabasin flow from the northwest and from the north (Winograd and Thordarson, 1975). Due to high evapotranspiration rates for the Amargosa Desert, most of the recharge occurs through the ephemeral stream channels (Osterkamp et al., 1994; Savard, 1995). Since the stream channels in the Amargosa Farms portion of the Amargosa Desert rarely have flow, the recharge estimates of Osterkamp et al. (1994) are about 0.5 percent of precipitation. Precipitation is generally between 100 and 200 mm for the Amargosa River basin (Osterkamp et al., 1994).

The groundwater contribution from the proposed YM repository area is a small portion of the southward flow along Fortymile Wash. The contribution from the Ash Meadows springs area to the Amargosa Farms area may be minimal. The Ash Meadows springs line and high gradient toward the Amargosa Farms area is a reflection of the hydraulic conductivity contrast across a gravity fault which abuts the carbonates of Ash Meadows on the east side with the confining playa deposits on the west side (Naff, 1973).

3 WELL CONSTRUCTION AND WATER USE IN THE AMARGOSA FARMS AREA

Characterization of well construction practices and water use specific to the Amargosa Farms area is presented in this section. Some aspects have been presented elsewhere (e.g., U.S. Department of Energy, 1988) but either the level of detail was not sufficient or data were included for other areas of the Amargosa Desert region.

Four sources of information were used to characterize well construction and water use in the Amargosa Farms area. The well permit database, well driller's logs, and annual water use estimates were obtained from the Nevada Division of Water Resources (Nevada Division of Water Resources, 1997a,b,c; Bauer and Cartier, 1995). A fourth source was the Ground-Water Site Inventory (GWSI) portion of the National Water Information System developed and maintained by the U.S. Geological Survey (USGS) (U.S. Geological Survey, 1989). The well permit tables, well driller's logs, and annual water use tables are recorded by location using the standard range, township, section, quarter section, and possibly quarter-quarter section coordinate system. The tables are organized by hydrographic basin with the Amargosa Desert being defined as basin 230. The Amargosa Farms area of the Amargosa Desert includes townships (T) 15, 16, and 17 south (S) and ranges (R) 48 and 49 east (E), as well as the western half of R50E.

The GWSI database uses both the township-range coordinate system as well as the longitude-latitude coordinate system. The wells in Amargosa Farms and Amargosa Valley are taken as those bounded by $-116^{\circ} 21' 34''$ to $-116^{\circ} 37' 15''$ west longitude and $36^{\circ} 40' 10''$ to $36^{\circ} 20' 53''$ north latitude. For graphical purposes, township-range coordinates and latitude and longitude coordinates are converted to UTM section 11 coordinates using the NAD27 datum. The former conversion is made directly to UTM by assuming a well is in the middle of the smallest reported area (e.g., quarter section). The latter conversion is made using a USGS-supplied conversion program.

3.1 NUMBER AND DISTRIBUTION OF WELLS

A division of wells into two categories based on water use is made here for the purpose of presentation of separate results for different receptor pathways. Domestic and quasi-municipal wells can be characterized as having low but continuous pump rates throughout the year. Irrigation wells and commercial and industrial wells constitute the large pump rate category. Although irrigation wells operate intermittently through the growing season, they are approximated in this study as a continuously pumping well at the annual rate estimated from the annual volume pumped.

There are no municipal wells in the Amargosa Farms area. Instead, quasi-municipal wells and domestic wells support direct human use. In addition, a portion of the irrigation wells (well driller's logs) and industrial wells (Buqo, 1996) may also supply water for direct human use. Five percent of the total irrigation wells recorded in the well driller's log also listed domestic use. Dependent on the State Engineer's concurrence, the water use category associated with a permit may be changed at a later date.

There are 508 wells recorded in the State of Nevada's well driller's logs which date back to at least 1921. Many of these wells are no longer in operation. The GWSI database contains 224 well records for approximately the same area of central Amargosa Desert. The well permit database contained 185 certificated or permitted water rights entries. The estimated water use tables from the Nevada State

Engineer tracked as many as 72 entries in one year (1996) and a combined 126 different entries over the span 1983–1996. Individual domestic wells are not recorded in the state water use tables, nor were quasi-municipal wells prior to 1996 for Hydrographic Basin 230.

The distribution of wells spatially and across water use categories is illustrated in table 3-1 by Township and figure 3-1 by Range and Township. The U.S. Department of Energy (DOE) (1988) identifies nine quasi-municipal wells, five commercial wells, and three industrial wells that were active. Changes in water use category may occur on permitted or certificated water rights. A majority (70 percent) of all wells were drilled in T16S. Figure 3-1 shows that the domestic wells are concentrated in T16S and R48-49E. Locations of sections where 14 or more (up to 40) domestic wells have been drilled according to the well drillers logs are also marked in figure 3-1.

3.2 STATISTICAL ANALYSIS OF WELL CONSTRUCTION PRACTICES

The GWSI database (U.S. Geological Survey, 1989) also contains information on well construction. Of the 227 wells from the Amargosa Farms region listed in the database, 188 records included water table depth, 113 included screen positions, and 15 records included specific discharge data. Although 18 wells had multiple screened portions, a majority of the screened portions are closely spaced. This is reflected in the fact that there is only a 1-m difference between the average of the sum of the screened portions and the average of the length of the combined screened portion. Table 3-2 is a statistical summary of relevant well characteristics. Of note are the averages of 11 and 62 m depths from the water table to the top and bottom of the screened portions, respectively.

3.3 ESTIMATION OF WATER USE

For the Amargosa Desert, designated as Hydrographic Basin 230, the state has estimated the perennial yield to be 24,000 acre-ft-yr (Buqo, 1996). Committed water use, which includes both certificated and permitted water use, is over 41,000 acre ft-yr. This situation makes it unlikely that new permits will be granted by the State Engineer. In the past few years, proceedings for water users to demonstrate beneficial use have led to thousands of acre-feet of forfeiture for well permits. These proceedings may have had an impact on the number of water users reported in the basin during the mid-1990's (Buqo, 1996).

On a volume basis, the water pumped in the Amargosa Farms region is predominantly used for irrigation and mining. The bulk of the mining related water use is in the playa area, which lies south of the farming area. The St. Joe Bullfrog Gold Mine is also a large-volume water user as reported in the tables for the Amargosa Desert but it is not located in the Amargosa Farms region. Historically, groundwater pumping for irrigation increased significantly in the late 1950's (D'Agnese, 1994; and Buqo, 1996). Irrigation use was 3,000 acre-ft by 1962, 9,300 acre-ft by 1967, and 7,300 acre-ft in 1973. Kilroy (1991) reports rapid declines in the water table during the 1970's and less severe declines in the 1980's. The declines are 20 to 30 ft in three different areas of Amargosa Farms with the largest being a northeast-trending trough near the Nevada-California border in T16S, R48E.

Since 1983, the Nevada State Engineer has tabulated water use for individual users and summarized annual use by category, although data for 1984 were not recorded. Table 3-3 is the annual summary of water use with both the Amargosa Desert total and the Amargosa Farms portion total. The

Table 3-1. Distribution of wells by water use across Townships T15,16,17S using well driller's logs. There are 34 log entries classified as other. See figure 3-1 for layout of Townships and Ranges.

Township	Domestic	Irrigation	Industrial/ Commercial	Quasi- Municipal
T15S	12	5	2	1
T16S	207	120	1	3
T17S	55	65	1	1

Table 3-2. Statistics for well construction practices and water level positions for wells recorded in GWSI database in Amargosa Valley and Amargosa Farms area

Well Characteristic	Average	Standard Deviation	Number	Minimu m	Maximu m
Distance from Water Level to Top of Screen (m)	11	13.0	113	0	66.0
Distance from Water Level to Bottom of Screen (m)	62	36.7	113	1.7	219
Distance from Water Level to Screen Centerline (m)	35	23.1	113	1.2	124
Total Screen Length (m)	52	33.2	113	0.9	191
Distance from Top to Bottom of Screens (m)	53	33.1	113	0.9	191
Depth of Well (m)	83	42.6	172	0.9	229
Wellbore Diameter (m)	0.31	0.08	112	0.032	0.41
Specific Discharge (m ² /hr)	32.3	33.4	15	2.34	104

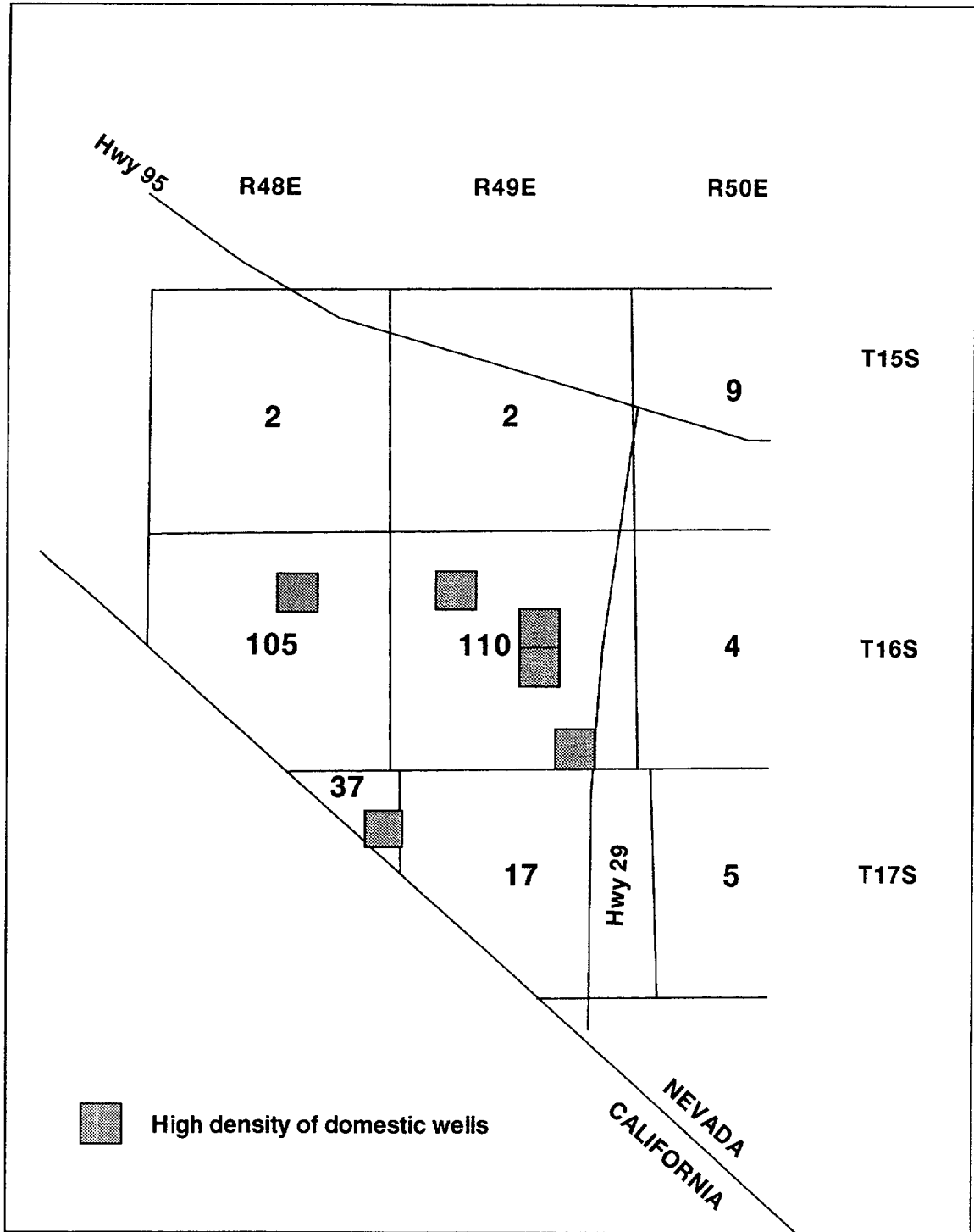


Figure 3-1. The distribution of domestic and quasi-municipal wells based on range and township from well driller's logs. The number of wells in each range and township includes those listed for dual usage, domestic, and irrigation. Locations of sections (1 square mile) with 14 or more domestic wells are highlighted.

Table 3-3. Annual estimates of water use by type; International Minerals Venture Floridan (IMV), American Borate (AB), quasi-municipal (QM), commercial (COM)

Year	Basin-230 Total Acre-ft	Irrigation Acre-ft	IVM/AB Acre-ft	QM/COM Acre-ft	Domestic Acre-ft	Amargosa Farms Total Acre-ft
1996	13,613	11,033	1,019	204	50	12,306
1995	15,035	12,354	780	10	100	13,244
1994	12,595	9,977	717	10	100	10,804
1993	11,300	8,659	1,007	10	100	9,776
1992	8,164	5,711	654	10	100	6,475
1991	6,122	4,942	450	10	100	5,502
1990	7,807	4,953	887	10	125	5,975
1989	3,921	1,566	1,413	10	125	3,114
1988	4,109	2,978	996	10	125	4,109
1987	6,137	5,700	302	10	125	6,137
1986	7,238	6,553	550	10	125	7,238
1985	9,672	8,472	950	20	230	9,672
1983	9,500	9,105	125	20	230	9,500

annual totals increased significantly from 1993 to 1996 due to large increases in irrigation use with the largest volume being 13,244 acre-ft in 1995.

Individual domestic water use is not recorded in the State Engineer's tables, and individual records for quasi-municipal water users did not start until 1996. Annual estimates were lumped together for the domestic and quasi-municipal/commercial use for each year, although there is some recategorization occurring in 1996. A 1 acre-ft annual usage is assumed for every household, although this may be an over-estimate (Buqo, 1996). However, the DOE (U.S. Department of Energy, 1988) states that the annual household usage estimate is 1,800 gpd. One acre-ft is about 895 gpd or about 3.4 m³/d.

Individual records for each irrigation user are tabulated (appendix A) for the years 1983, 1985-1996 and pertinent summaries are included in table 3-4. For individual users, the maximum annual pump volume for any particular user is 3,960 m³ (1,170 acre-ft). The average for all years for an individual irrigation user is 828 m³ and the range in any particular year is 348 to 1,300 m³. The number of irrigation users for any year ranged from 15 in 1991 to a high of 55 in 1996. Most of the groundwater

Table 3-4. Summary statistics of individual irrigation users on an annual basis

Year	Average (m ³ /d)	Number of Users	Minimum (m ³ /d)	Maximum (m ³ /d)
1996	772	55	3.4	2,707
1995	886	51	6.8	2,928
1994	771	44	3.4	3,960
1993	711	41	3.4	3,960
1992	645	30	3.4	3,368
1991	1116	15	67.7	3,960
1990	645	26	16.9	2,675
1989	348	16	16.9	1,354
1988	503	20	8.5	2,370
1987	900	20	8.5	2,912
1986	1300	17	8.5	2,928
1985	1134	25	76.9	2,928
1983	1083	26	16.9	2,116
Overall	828	—	—	—

pumping occurs in T16S, R48-49E, and T17S, R49E. Figure 3-2 shows the distribution of groundwater pumping for the year 1996 by township and range based on the individual records (no domestic wells are recorded). Figure 3-3 shows the distribution for 1996 relative to the streamtube model boundaries used in Baca et al. (1997). In combination, figures 3-2 and 3-3 illustrate two important points based on 1996 data. One, domestic or quasi-municipal wells are likely to be the first wells encountered by a plume migrating from the proposed YM repository. Two, large pumping rate wells capable of capturing a plume are not encountered until about 30 km from the proposed YM repository.

In summary, the typical pump rates range from 300 to 2,000 m³/d for irrigation wells and 3 to 6.8 m³/d for domestic wells. Although the Hydrographic Basin of Amargosa Desert is over-appropriated, actual usage has remained less than 65 percent of the estimated perennial yield. Groundwater pumpage in the Amargosa Farms portion of the Amargosa Desert has led to a decline in the water table locally up to 10 m.

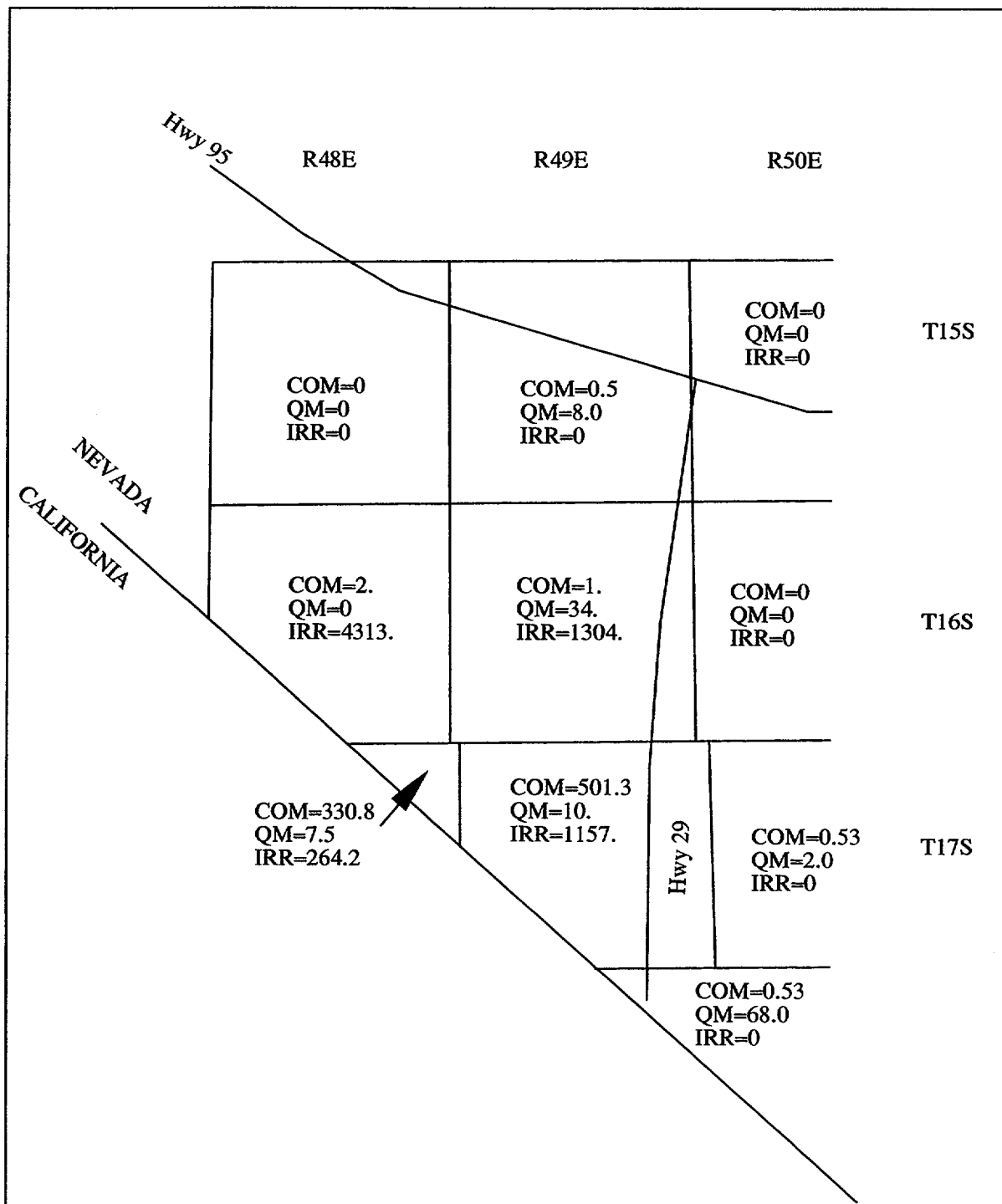


Figure 3-2. Distribution of annual water use (acre-ft) by type and by range and yownship for commercial, irrigation, quasi-municipal wells for the year 1996

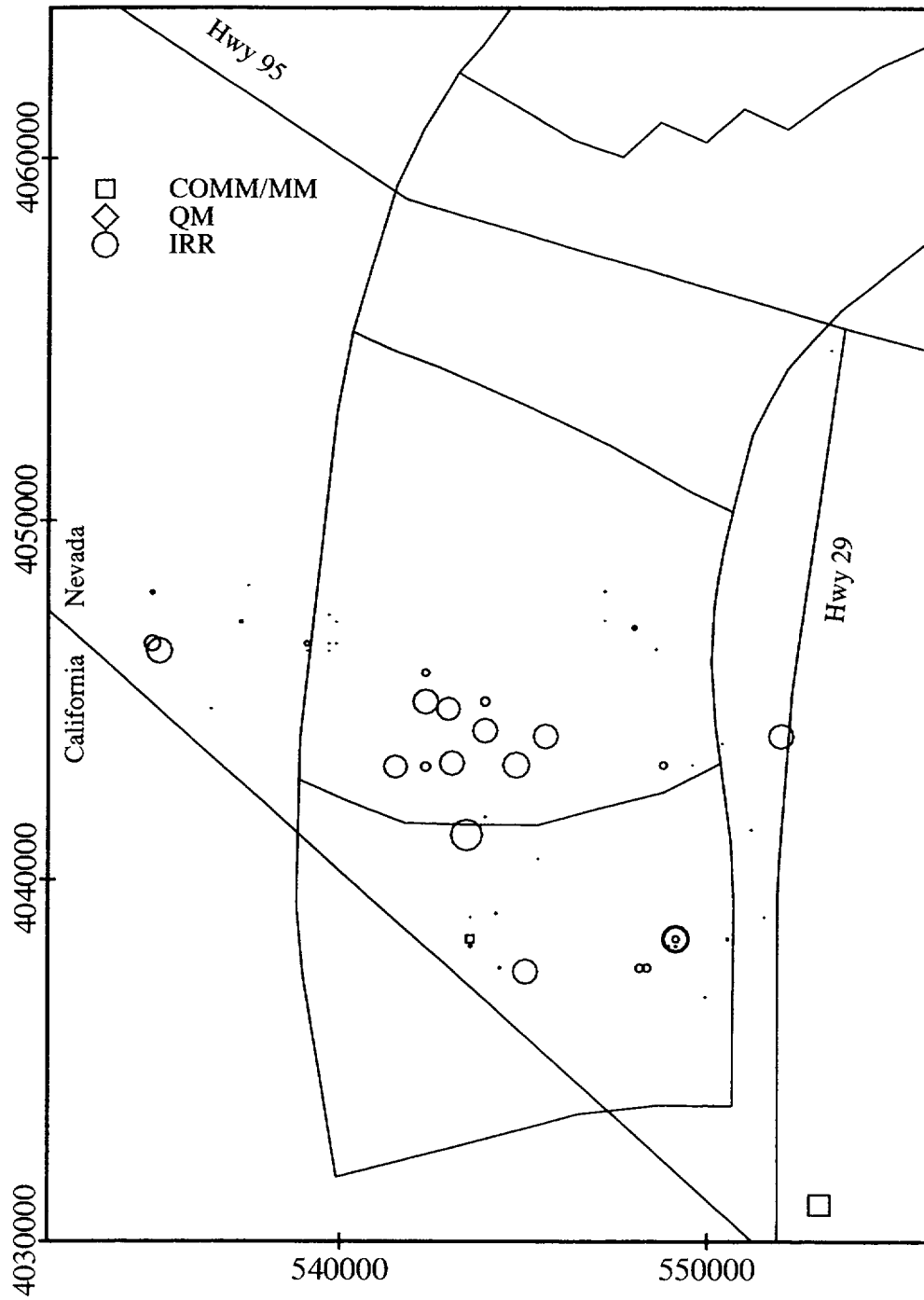


Figure 3-3. Distribution of water use by type for the year 1996. The symbol size for each category is scaled to the magnitude of groundwater pump volume. Data are from Nevada Division of Water Resources (1976b) and are converted to Universal Transverse Mercator Section II coordinates so as to correspond with the streamtube model of Baca et al. (1997).

4 THREE-DIMENSIONAL CAPTURE ZONE ANALYSIS AND PLUME DELINEATION

The approach used here to estimate borehole dilution factors in the Amargosa Farms region is to separate them into two components; one, the factor due to volumetric-flux; and two, the factor due to dispersion during transport. The factor due to volumetric flux is a comparison of the cross-sectional areas of a capture zone of a pumping well to the intercepted portion of a contaminant plume. In all cases, the areas discussed here refer to the cross-sectional area normal to the principal direction of regional flow. The second component of borehole dilution is the effect due to dispersion during transport. It is calculated as the ratio of the source concentration to the areal average concentration of the portion of the plume which is captured by a pumping well.

Other types of dilution factors include that used by Baca et al. (1997) and Kessler and McGuire (1996) based on normalized concentration variations during passive transport, and that used in IPA Phase 3 based on a mass release rate into a total volumetric flux potentially used by a critical group. The dilution factor due to dispersive transport used in this report accounts for the distribution of concentration across a plume whereas that used by Kessler and McGuire (1996) only accounts for concentration reduction along the centerline of the plume. Direct usage or comparison of the borehole dilution factor and the IPA Phase 3 dilution factor is restricted by the reference to different volumetric fluxes.

Different configurations for the intersection of the plume and the capture area are possible. For domestic wells, the capture area is generally much smaller than the cross-sectional area of a plume that has undergone transverse spreading due to macro-dispersion during transport along a 20- to 30-km pathway (figure 4-1). Hence, there would be little borehole dilution even if the well was aligned along the center of the plume, and any borehole dilution that did occur would be due to vertical gradients in the plume concentration. For a 2D plume of prescribed thickness, the location of the plume relative to the capture area affects the dilution factor. For irrigation wells, or any high discharge wells, the capture area is generally thicker than the plume. The capture area may be wider or narrower than the contaminant plume depending on the problem. In all cases, the well is assumed to be in the transverse center of the plume which is the conservative assumption.

The effects of the regional gradient, transmissivity, pumping rate, and screen position and length on the area of the capture zone can be described in qualitative terms. An increase in transmissivity or the regional gradient will decrease the width of the capture area. An increase in the pumping rate will increase the capture area. An increase in the depth of a partially penetrating well will increase the vertical capture area but decrease the horizontal capture area. The position and distribution of the plume in relation to the capture zone will control the dilution of the solute in the well bore.

At present, there are few data for the hydraulic properties, well construction, and pumpage in the Amargosa Desert or Amargosa Farms. Moreover, the size, location, and shape of a plume are uncertain and usually must be obtained from large-scale transport modeling. Because of the relative paucity of site-specific data, the focus of this study is relating dilution trends to generic well design and plume configuration.

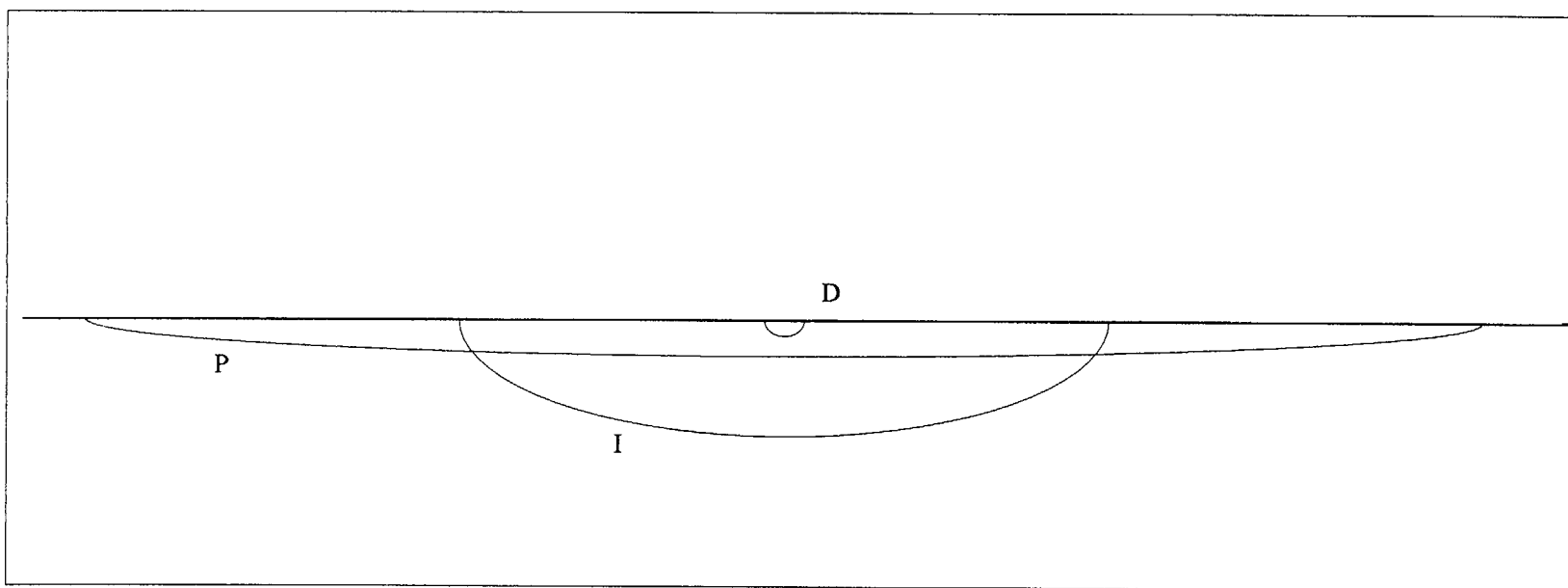


Figure 4-1. Comparison of plume cross-section (P), irrigation well capture area (I), and domestic well capture area (D)

4.1 DETERMINATION OF FLOW FIELD AND CAPTURE ZONE

The groundwater flow simulation program GFLOW Version 1.1 (Haitjema, 1995), that is based on the analytic element method, was used to estimate the size and shape of capture zones for individual wells. GFLOW is designed to simulate partially penetrating wells in a uniform regional gradient. There are other types of elements in GFLOW for modeling groundwater flow fields that were not used. The 3D effects of the partially penetrating well are superimposed on the 2D regional flow field. At some distance from the well, the vertical components due to pumping become negligible. Forward or backward particle tracking is used in GFLOW to determine a capture area at some distant, upgradient point where vertical flux components become insignificant. This capture area is a vertical plane normal to the direction of regional flow.

4.1.1 Description of the Analytic Element Method

The Analytic Element Method (AEM) provides a composite analytic solution which satisfies the differential equation in an unbounded domain. Delineation of streamlines is more precise than with standard numerical methods since both the head and the velocities are known at every point, rather than solely at computational nodes. Combined 2D and 3D modeling is accomplished by superposition of 3D effects on the general 2D solution. For example, near a partially penetrating well, a 3D solution is used. However, at a location sufficiently far from the well, the vertical flow components are negligible and a 2D approximation to the well may be superimposed on the solution. AEM is not well suited for complex flow problems in which material property heterogeneity is large.

The equations for flow in AEM are written in terms of discharge potentials instead of hydraulic head. The discharge potential is defined differently for confined, unconfined, 1D flow, 2D flow, or for any analytic element. An advantage of the AEM is that the solution to the equation for flow written in terms of the discharge potential is not dependent on whether the problem domain being solved is confined or unconfined. Once the strength of the potential is known for each analytic element, the head or groundwater discharge may be determined at any point in the flow domain. The solution for the partially penetrating well is based on work by both Muskat and Polubarinova-Kochina (Haitjema, 1995) for the representation of the strength distribution along a line sink (point sinks along a line) while constraining the discharge to a fixed value.

4.1.2 Ranges for Parameter Values

Four parameters are varied to test their effects on the capture area including: (i) pump rate, (ii) well screen position and length, (iii) regional gradient, and (iv) hydraulic conductivity or transmissivity. The pump rates range from those typical of domestic wells to those typical of irrigation wells. A reasonable range to use for the pump rates for domestic or quasi-municipal wells is 1 to 75 m³/d. The DOE estimate (U.S. Department of Energy, 1988) for a single household is 1,800 gpd (6.8 m³/d) while the State of Nevada uses 1 acre-ft per household (3.4 m³/d) noting that this value is probably too high (Buqo, 1996). The high end of the domestic range corresponds to a quasi-municipal well or to multiple domestic wells modeled as a single well. For example, the first wells in a potential plume's path are multiple domestic, quasi-municipal, and small commercial wells near the junction of highways 95 and 29 at Amargosa Valley. For irrigation wells, pumping may be as high as 4,000 m³/d; however, a more typical large irrigation pump rate is 2,116 m³/d (625 acre-ft/yr). The average pump rate from 1983–1996 was about 800 m³/d while the lowest was 300 m³/d for any particular year.

The average screened length of the wells in the Amargosa Farms region (top to bottom) is 53 m while the maximum screen length is 190 m (table 3-2). The typical screen position starts 11 m below the static water level at the time of construction. Hence, the typical well modeled here will be screened from the water table to 60 m below the water table. Sensitivity analysis for the screen position, for domestic wells only, will account for the adjustment steps of about one standard deviation of the screen position.

The range of regional hydraulic gradients considered is 0.01 to 0.001. Bedinger et al. (1989) list a value of 0.003 for generic basin-fill environments in the Death Valley Region. Estimates for the Amargosa Farms area made from water table maps by Kilroy (1991), the DOE (U.S. Department of Energy, 1988), and Nichols and Akers (1985) fall within the 0.001 to 0.01 range. Most estimates are in the 0.001 to 0.005 range; the 0.01 values are from the east-west gradients immediately south and east of Amargosa Valley and may reflect the abrupt decrease in transmissivity across the northern end of the so-called Gravity fault, which has been inferred along the Ash Meadows spring line.

The range of transmissivities reported for basin-fill alluvium in the Death Valley Region is 10 to 400 m²/d (Plume, 1996; U.S. Department of Energy, 1988; and Winograd and Thordarson, 1975). Since Amargosa Farms is in the area of sediments facies of lower fans and lowland sediments, rather than the coarser sediments of the upper and middle fan deposits, the saturated hydraulic conductivities should encompass a wide range and be highly heterogeneous relative to other basin-fill. Plume (1996) estimates a range of 0.006 to 43 m/d for saturated hydraulic conductivity while the DOE (U.S. Department of Energy, 1988) reports a range of 0.21 to 2.9 m/d. The transmissivity is a product of the saturated hydraulic conductivity and the saturated thickness of the aquifer. The aquifer thickness is assumed to be 1,000 m for all modeling scenarios.

4.1.3 Sensitivity Analysis for Capture Zone

The effects of reasonable variations in transmissivity, regional gradient, and pumping rate for all well types are presented in this section. In addition, the effects of screen position and length for domestic wells are presented. Due to their large discharge rates and small degree of well penetration relative to the aquifer thickness, the effects of screen position and length are negligible for irrigation wells. The capture area is determined at an upgradient point from the well location where the flow is essentially 1D, for example, no longer 3D. At this upgradient point, the width and thickness are at a maximum for the capture area. A table of the widths and depths of the capture area results is included in appendix B.

The effect of a partially penetrating well compared with that of a fully penetrating well is shown in figure 4-2 for a small irrigation well pumping at 300 m³/d. The maximum screen length of 190 m is marked as maximum on the figure. The capture width of the fully penetrating well is about 44 percent of that for the typical partially penetrating well.

Figure 4-3 represents the capture zone width and thickness for combinations of regional gradients and transmissivities for a large pumping rate well of 2,116 m³/d (625 acre-ft/yr). The combination of a regional gradient of 0.001 and transmissivity of 200 m²/d (the lowest represented here) leads to a capture width of about 5,600 m, which captures nearly the entire width of a streamtube (Baca et al., 1997) that brackets the repository. Conversely, a larger gradient (0.005) and higher transmissivity (400 m²/d) lead to a much smaller capture area, 1,800 m wide by 720 m deep. A similar trend also occurs for low-discharge, domestic wells (figure 4-4). Maximum capture areas are created either by the smallest regional gradient (0.001) or the lowest transmissivity (10 m²/d) for capture thicknesses up to

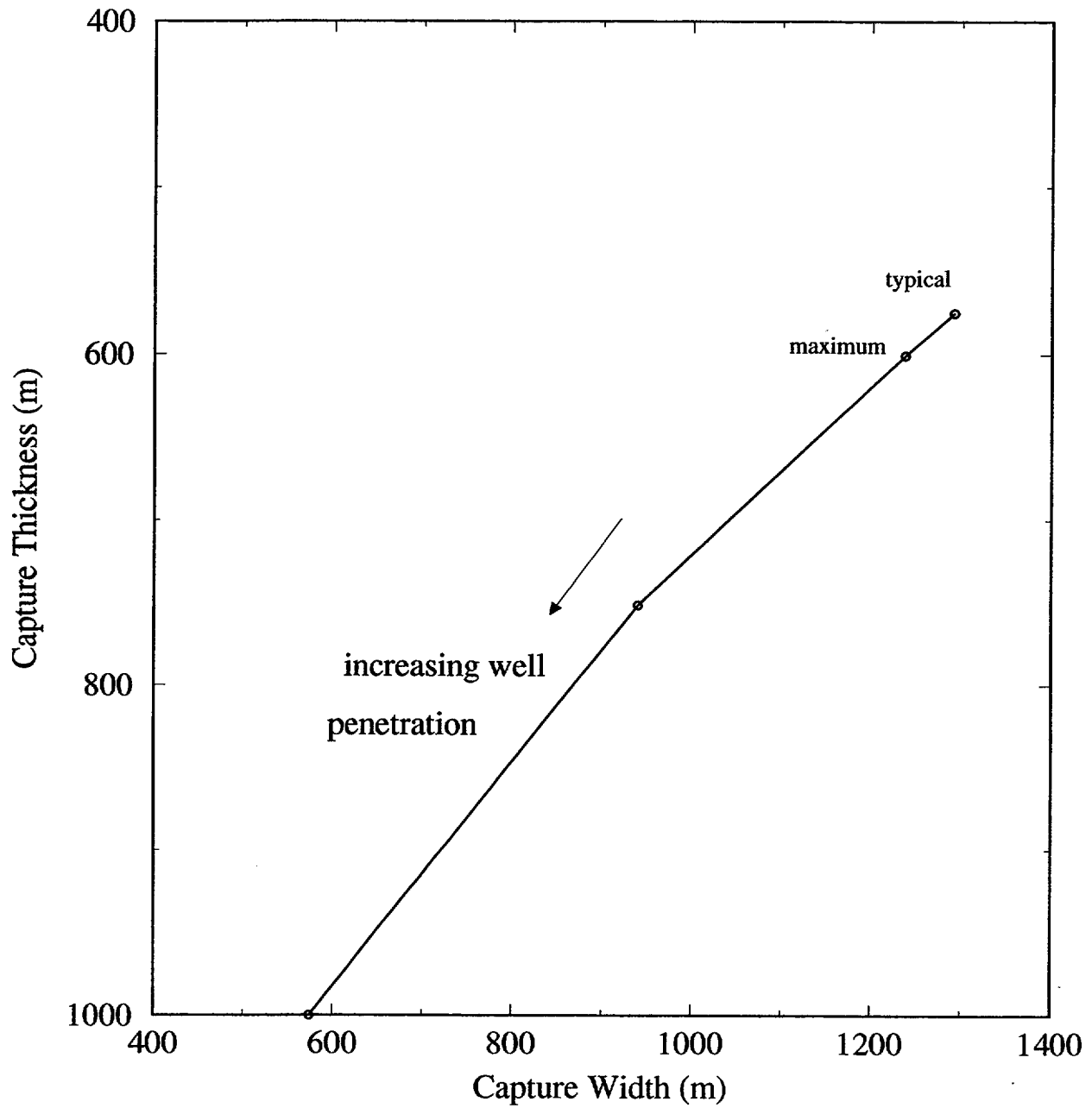


Figure 4-2. This plot illustrates the effect of well penetration depth (60, 190, 500, and 1,000 m) on a small irrigation capture zone width and thickness. A pump rate of 300 m³/d and regional gradient of 0.005 are used. The “maximum” denotes the maximum well penetration depth and “typical” denotes the typical well penetration depth for the Amargosa Farms region.

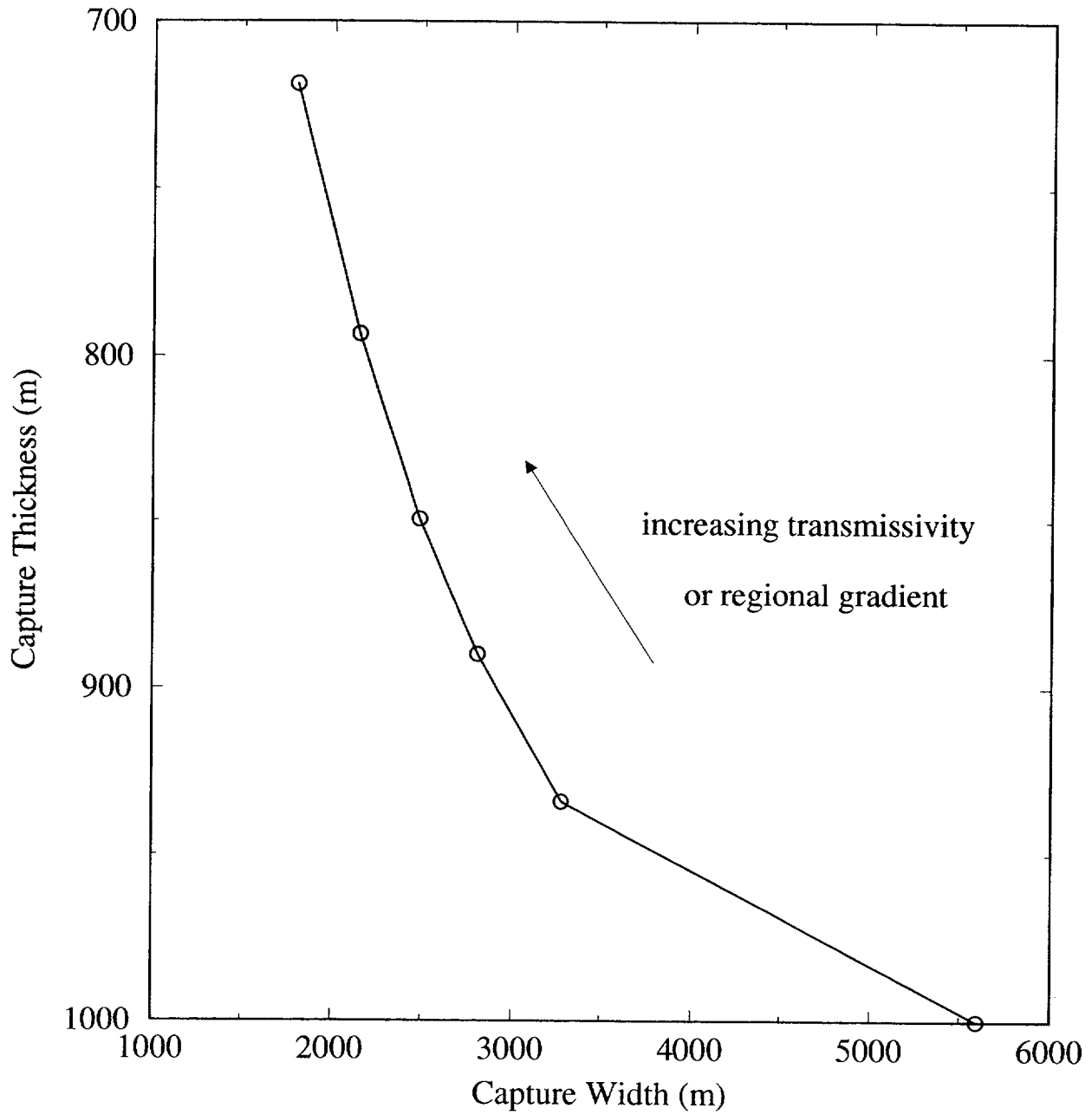


Figure 4-3. Effect of combinations of transmissivity (200, 300, 400 m²/d) and hydraulic head gradient (0.001, 0.002, 0.003, 0.005) on a large irrigation well's capture zone width and thickness. A pump rate of 300 m³/d is used.

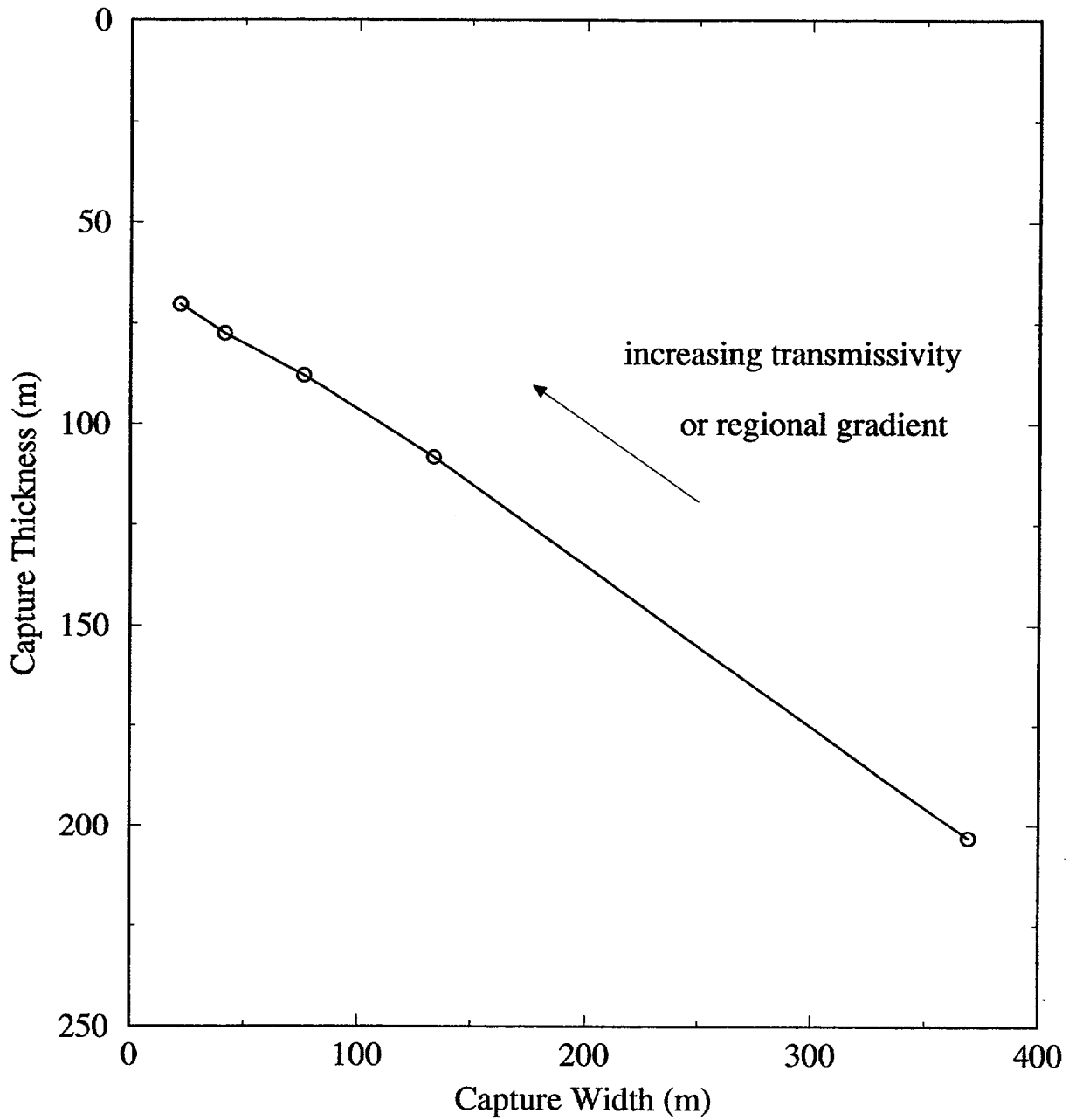


Figure 4-4. Effect of combinations of transmissivity (50, 100, 200, 300, 400 m^2/d) and hydraulic head gradient (0.001, 0.0025, 0.005, 0.01) on a domestic well's capture zone width and thickness. A pump rate of 3 m^3/d and the screened portion is 60 m long starting from the water table.

200 m. Since the Darcy velocity is a function of the hydraulic conductivity and hydraulic gradient, figures 4-3 and 4-4 also illustrate the effect of Darcy velocity on capture width and thickness.

The effect of pump rate on the capture area is presented in figure 4-5. A gradient of 0.005 and transmissivity of 100 m²/d are used for all pump rates. Of significance for borehole dilution is that all wells in the low pump rate range (<75 m³/d) will have capture areas that would be much less than the plume area based on 3D advection-dispersion equation modeling.

4.2 RADIONUCLIDE PLUME SHAPE AND LOCATION

The potential release and subsequent movement of radionuclides from the YM repository is likely to follow a path generally southeast to Fortymile Wash and then continue south to southwest toward the Amargosa Valley and Amargosa Farms areas. A more precise delineation of the flow path under current conditions is a point of debate due to a lack of data and the absence of any detailed hydrogeologic study in the Fortymile Wash and lower Amargosa Desert areas. The shape of the plume at a 30-km distance from the proposed repository, in particular the amount of vertical dispersion which leads to an increase in the plume thickness, is yet another unknown. Vertical dispersion may be limited by the possible presence of confining horizons (Naff, 1973) in the lake bed facies of the basin-fill sediments.

Given the uncertainty of the plume configuration, two scenarios were analyzed. The first scenario was a plume modeled for 3D dispersion. The second scenario is a plume for which no vertical dispersion is incorporated. Both scenarios are simulated to a steady state solution to assess the maximum dimensions of a plume reaching a well.

Dispersion, adsorption, and radioactive decay of the radionuclides will occur along this transport path. Adsorption and decay depend on the particular radionuclide. However, most of the radionuclides of concern in the far field (e.g., ²³⁷Np, ¹²⁹I, ⁹⁹Tc) have half-lives greater than 10,000 yr. Adsorption also depends on the surface mineralogy of the porous media as well as the chemistry of the groundwater. There are no site specific data for adsorption in terms of distribution coefficients for the valley fill sediments. Considering these points, the conservative approach of neglecting both decay and adsorption is adopted.

In order to evaluate dilution due to both vertical and horizontal capture of clean water by a pumping well, an estimate of the shape of a potential plume is needed. Specifically, the configuration of the cross-sectional area perpendicular to the direction of flow is needed. Analytic solutions to the advection-dispersion equation were previously used to describe the plume shape at downgradient points from YM in TSPA-95 (TRW Environmental Safety Systems, Inc., 1995 and Kessler and McGuire, 1996). The advection-dispersion equation for 3D dispersion and 1D flow is

$$\frac{\partial C}{\partial t} = D_x \frac{\partial^2 C}{\partial x^2} + D_y \frac{\partial^2 C}{\partial y^2} + D_z \frac{\partial^2 C}{\partial z^2} - V \frac{\partial C}{\partial x} \quad (4-1)$$

where C is the concentration, D_x , D_y , and D_z are the dispersion coefficients in the coordinate directions, V is the seepage velocity in the principal direction of flow, and t is time.

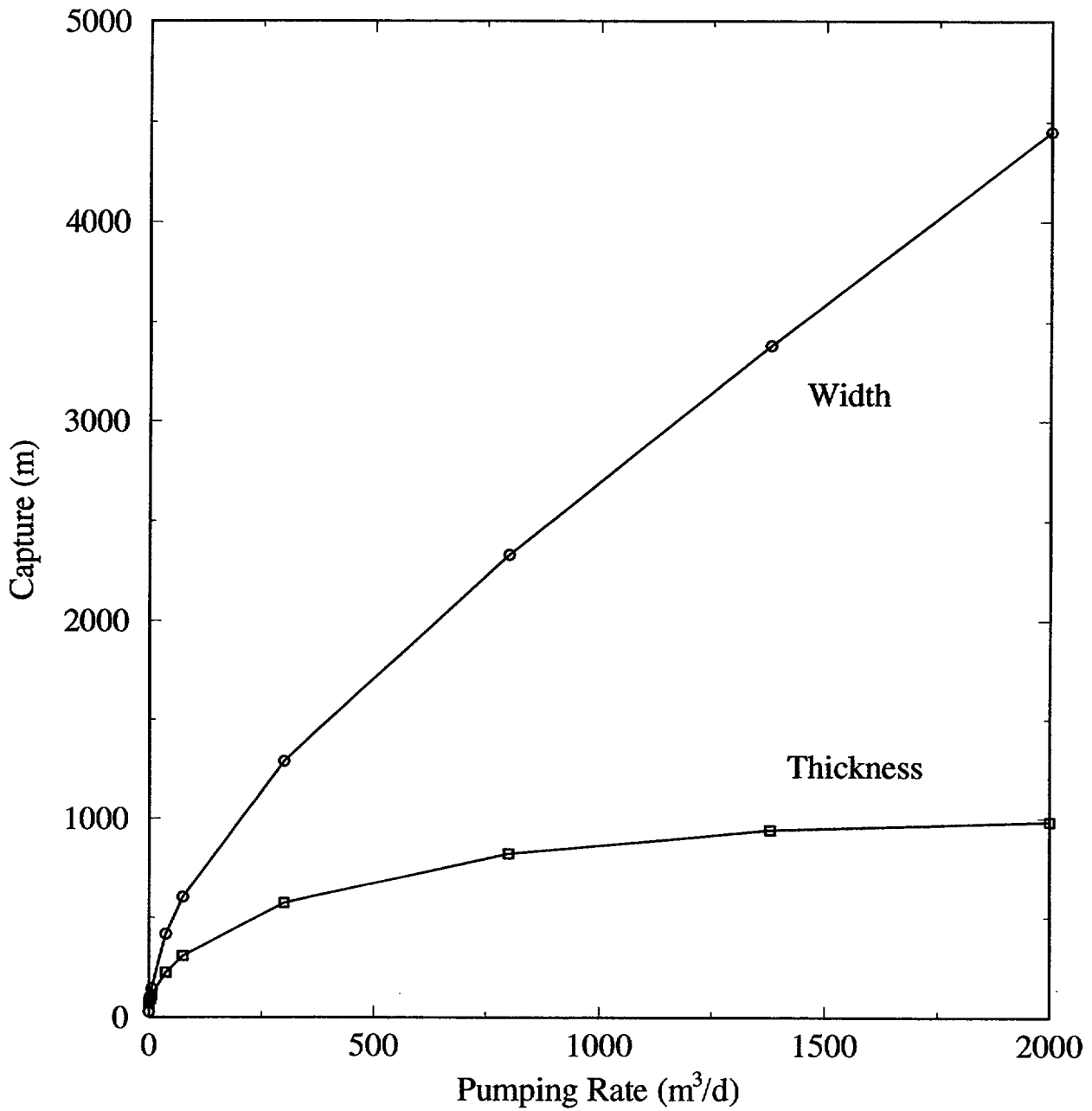


Figure 4-5. This plot illustrates the effect of pump rate (range 1 to 2000 m³/d) on the capture zone width and thickness. A transmissivity of 100 m²/d and regional gradient of 0.005 are used.

4.2.1 Transport Parameters

The initial source size, seepage velocity, and the dispersivities all control the plume configuration after 30 km of advective-dispersive transport. Kessler and McGuire (1996) noted the inverse relationship between source size and mean concentration reductions. They also found that a doubling of the source thickness led to an increase of 17 percent in the plume width at 25 km. Similarly, a 60-percent increase in the source width led to an increase of 6 percent in the plume width at 25 km. In this study, the source size will be held constant at 500 by 25 m for the 3D dispersion plumes and 500 m wide for the 2D dispersion plumes.

Since transport simulations were run to steady state in order to determine maximum plume dimensions, a reasonable value of the seepage velocity along the flow path from the repository, or from the accessible environment, to Amargosa Farms is needed. Seepage velocity is related to the Darcy flux by porosity. The Darcy flux for the transport analysis need not be the same as that for the capture zone analysis since the former represents the porous media and hydraulic head gradients from the repository to Amargosa Farms while the latter represents the Amargosa Farms area. Seepage velocity for transport was chosen to represent the mean pathway velocity from the tuff through the alluvium. Baca et al. (1997) report calculated ranges of Darcy flux of 0.01 to 3.7 m/yr for the saturated tuff aquifer and 0.4 to 0.7 m/yr for the alluvium. Assuming a porosity of 0.3 for the alluvium, the seepage velocity would be in the range of 1.3 to 2.3 m/yr. Kessler and McGuire (1996) used a seepage velocity of 1.76×10^{-6} m/s (55 m/yr) although it is not clear whether site-specific information (gradient, hydraulic conductivity, porosity) was used to obtain this estimate. The value of 2.4 m/yr used here for seepage velocity is closer to that approximated from the Darcy flux values reported by Baca et al. (1997).

The value of the concentration at the source is chosen to approximate a mass release rate of 10 Ci/yr, which is taken as an upper bound for mass release rates as delineated by the ^{99}Tc example in Mohanty et al. (1997). Assuming that dispersion off the constant concentration boundary is negligible, the concentration corresponding to 10 Ci/yr is $4.38\text{E}-6$ Ci/l for a source size of 500 by 25 m and a Darcy velocity corresponding to a seepage velocity of 2.4 m/yr with a porosity of 0.3. The assumption of negligible dispersion off the source boundary as compared to advective flux off the boundary is reasonable at long times. However, since the plume configurations scale directly for steady state problems, the value of the concentration at the boundary conditions does not affect dilution factor estimates; as long as normalized values of concentration are reported and not absolute concentrations.

Simulation of 3D dispersion requires values for the longitudinal, horizontal transverse, and vertical transverse dispersivities. Generally, dispersivities are considered to be scale dependent (Gelhar et al., 1992). TSPA-95 (TRW Environmental Safety Systems, Inc., 1995) assumed relatively large transverse dispersivities which resulted in exceptionally large plumes (especially in the vertical direction) and large dilution factors (10^3 to 10^5). Kessler and McGuire (1996) recognized that there is a limit to the heterogeneity scale that a plume would encounter, although they nonetheless used a vertical transverse dispersivity equal to the horizontal dispersivity. This seems unlikely in light of the lithologic layering in the alluvial basin sediments. Contaminant plumes generally exhibit limited vertical spreading (Gelhar et al., 1992). Thus, small vertical transverse dispersivities values are likely. In a literature review of measured dispersivity values and ratios, Gelhar et al. (1992) note that horizontal to vertical transverse dispersivity ratios are often 1–2 orders of magnitude different. Furthermore, the measured vertical dispersivity values were all reported in Gelhar et al. (1992) to be less than 1 m; generally, in the range 0.06 to 0.3 m for scales ranging from 20 m to 10 km. In addition, the vertical transverse dispersivity

values exhibited no scale dependency. The longitudinal and horizontal transverse dispersivity are scale-dependent with their ratio equal to one order of magnitude. For the constant concentration source, the longitudinal dispersivity and the velocity do not affect the mean plume concentration in steady state transport. Plume size is controlled by the transverse dispersivities.

In this study, the location of the radionuclide source area is the same as that assumed by Kessler and McGuire (1996). A patch source area aligned perpendicular to the flow direction is located at the edge of the accessible environment or fence as described in Kessler and McGuire (1996), as opposed to locating the source area at the repository. The conceptual model consists of a release from the repository reaching the accessible environment from where it is modeled as a patch source to obtain a plume configuration 15 to 25 km further along Fortymile Wash to the Amargosa Farms area. Noting the variations in the flow path lengths, the accessible environment is approximately 5-7 km from the repository, the quasi-municipal and domestic wells first encountered at Amargosa Valley are about 15 km from the accessible environment, and the majority of irrigation wells first encountered are at about 25 km from the accessible environment.

4.2.2 Plume Dimensions for 3D Dispersion from Constant Concentration Source

The analytic solution to Eq. (4-1) for the constant concentration patch source as described in Wexler (1992) is

$$C(x,y,z,t) = \frac{C_0 x \exp\left[\frac{Vx}{2D_x}\right]}{8\sqrt{\pi D_x}} \int_0^t \tau^{-\frac{3}{2}} \exp\left[-\left(\frac{V^2}{4D_x} + \lambda\right)\tau - \frac{x^2}{4D_x\tau}\right] \left[\operatorname{erfc}\left(\frac{Y_1-y}{2\sqrt{D_y\tau}}\right) - \operatorname{erfc}\left(\frac{Y_2-y}{2\sqrt{D_y\tau}}\right) \right] \left[\operatorname{erfc}\left(\frac{Z_1-z}{2\sqrt{D_z\tau}}\right) - \operatorname{erfc}\left(\frac{Z_2-z}{2\sqrt{D_z\tau}}\right) \right] d\tau \quad (4-2)$$

where C_0 is the concentration at the source, τ is a dummy variable of integration for time, λ is the decay coefficient, \exp is the natural exponential, and erfc is the complementary error function. The dispersion coefficients in the x -, y -, and z -directions are defined as the products of the seepage velocity and the dispersivities in the x -, y -, and z -directions, respectively. This equation is the solution to the 3D solute transport equation for a vertical patch source aligned normal to the principal direction of flow where the patch dimensions are defined by $Y_2 - Y_1$ and $Z_2 - Z_1$. The solution to the advection-dispersion equation is valid for a 1D uniform flow field and 3D dispersion for a constant concentration source in an aquifer of infinite depth and lateral extent. Adsorption and radioactive decay of the solute are incorporated into the solution but were not used in this study. In the PATCH I Version 1.1 program, Wexler (1992) uses a Gauss-Legendre numerical integration technique to evaluate Eq. (4-2); however, possible round-off errors were reported for solutions at small distances and long times using this technique. For a similar problem, Domenico and Robbins (1985) simplify the integral problem by

summing over a specified number of continuous point sources in a patch. However, they too noted numerical errors at small distances and long times.

Tables 4-1 and 4-2 contrast plume width and thickness for various sets of dispersivity values at 15 and 25 km, respectively, from the source area located at the accessible environment. The longitudinal dispersivity value is reported in the tables but its magnitude is not a controlling factor for the results. The plume width and thickness are delineated at a threshold concentration of approximately $10^{-4} \times C_0$. The P-DF is also included in tables 4-1 and 4-2. These values will be used as a reference point for the dispersion-based dilution factors estimated in the following section. Where the centerline concentration can be used as a conservative estimate of the plume concentration, borehole dilution factors due to dispersion will be calculated by accounting for the distribution of concentration across a plume.

A reduction of the transverse dispersivities by 80 percent leads to a 46-percent reduction in plume width and thickness at 25 km. The ratio of the horizontal and vertical transverse dispersivities is kept at an order of magnitude. The percentages are approximately the same for the 15-km results. Similarly, a 50-percent reduction in the transverse dispersivities leads to a 24-percent reduction in plume width and thickness at 25 km.

4.2.3 Plume Dimensions Neglecting Vertical Dispersion for Constant Concentration Source

From the literature (Bedient et al., 1994), it is evident that existing plumes (caused either by accidental contamination or by deliberate injection of tracers for experimental purposes), typically show that plumes are often confined to a thin layer near the water table. Exceptions would occur in areas of high infiltration. The extreme case is to assume no vertical dispersion so the plume remains the same thickness as the source area but is dispersed laterally. This conceptual model for plume movement can be modeled using the following solution for 2D dispersion for a line source of specified width and constant concentration (Wexler, 1992):

$$C(x,y,t) = \frac{C_0 x}{4\sqrt{\pi D_x}} \exp\left(\frac{Vx}{2D_x}\right) \int_0^t \tau^{-\frac{3}{2}} \exp\left[-\left(\frac{V^2}{4D_x} + \lambda\right)\tau - \frac{x^2}{4D_x\tau}\right] \left[\operatorname{erfc}\left(\frac{(Y_1 - y)}{(2\sqrt{D_y\tau})}\right) - \operatorname{erfc}\left(\frac{(Y_2 - y)}{(2\sqrt{D_y\tau})}\right) \right] d\tau \quad (4-3)$$

The solution to Eq. (4-3) is implemented in the STRIPI Version 1.1 program of Wexler (1992). The solution for the line source can be extended to any source thickness.

In light of the arguments presented in the previous section, a reasonable selection of sets of dispersivities is 20:2, 50:5, and 100:10 for the longitudinal and transverse directions (table 4-3). These are depth-averaged dispersivity values which are not strictly comparable to the set of dispersivity values for 3D dispersion. When no vertical dispersion is included, the plume widths increase by between 16 and 29 percent for corresponding transverse dispersivities.

Table 4-1. Plume configuration and point dilution factor at 15 km from the source area for a range of dispersivity values. C_c is the centerline concentration. The source area is 25 m thick by 500 m wide.

$a_x:a_y:a_z$ (m)	Thickness (m)	Width (m)	P-DF = C_o/C_c
20:2:0.2	330	2,200	6
50:5:0.5	480	3,100	13
100:20:2	830	5,200	48
100:10:1	640	4,000	25
100:10:0.1	250	4,300	9

Table 4-2. Plume configuration and point dilution factor at 25 km from source area for a range of dispersivity values

$a_x:a_y:a_z$ (m)	Thickness (m)	Width (m)	P-DF = C_o/C_c
20:2:0.2	410	2,600	9
50:5:0.5	580	3,700	21
100:20:2	970	5,800	80
100:10:1	780	4,800	41
100:10:0.1	290	5,200	14

4.3 BOREHOLE DILUTION FACTORS BASED ON VOLUMETRIC FLUX

Volumetric flux-based borehole dilution factors (F-BDF) are determined by comparison of the plume and capture zone configurations (figure 4-1). The ratio of the cross-sectional area of the capture zone to the cross-sectional area of the portion of the plume which intersects the capture area in the plane perpendicular to the principal direction of flow is the dilution factor due to borehole mixing based on

Table 4-3. Plume configuration in terms of width at 15 and 25 km and point dilution factor for a source area width of 500 m and no vertical dispersion

$a_x:a_y$ (m)	Width (m) at 15 km	P-DF = C_o/C_c at 25 km	Width (m) at 15 km	P-DF = C_o/C_c at 25 km
20:2	2,330	1.5	2,860	1.8
50:5	3,410	2.1	4,230	2.6
100:10	4,640	2.8	5,800	3.6

volumetric flux comparisons. In other words, the F-BDF is the ratio of the capture and the intersection area. No credit is taken for the distribution of the concentration across the plume in the calculation of the F-BDF. All plumes in this section are modeled from a constant concentration source.

Generally, the plumes are wider than the capture zone but not as thick. Four plume scenarios are chosen to represent a range of conditions. The first and second scenarios are 10 m and 25 m thick plumes for which no vertical dispersion has occurred. The width of the plume depends on the horizontal transverse dispersivity that is used. For domestic wells, it does not matter what dispersivity is chosen since all plumes are wider than all domestic well capture zones. The third and fourth scenarios incorporate vertical dispersion with dispersivity ratios of 20:2:0.2 and 100:10:0.1. The F-BDF for the third and fourth scenarios are presented for the large pumpage irrigation wells.

4.3.1 Domestic Wells

The plume configuration that results from 3D dispersion from a constant concentration source will generally be larger than the capture area of a single domestic well, a closely spaced collection of domestic wells, or a quasi-municipal well for wells typical of the Amargosa Farms area. Hence, with the assumption of a uniform plume concentration, there will be no borehole dilution. Only for the smallest vertical transverse dispersivity values (less than 0.2) and for the largest pump volumes from a closely spaced collection of domestic and quasi-municipal wells will there be vertical gradients that are strong enough to capture clean water and provide borehole dilution.

The effects due to pumping rate, screen position, transmissivity, and regional gradient on the F-BDF are shown in figures 4-6 to figure 4-9. The plumes of thickness 10 and 25 m with no vertical dispersion are used for the calculation. As expected, the factors for the 10-m thick plume are greater than those for the 25-m plume. Again, the F-BDF do not include effects due to concentration differences in the plume.

For a typical domestic well that pumps 1,800 gpd, the F-BDF decreases from 10 to 4 when the plume thickness increases from 10 to 25 m at the 25-km distance (figure 4-6). The difference in the factors increases as the pumping rate increases. The F-BDF for the 10-m plume range between 7 and 26 for pumping rates in the range of domestic and quasi-municipal wells. Similarly, the F-BDF for the 25-m plume range between 3 and 10.

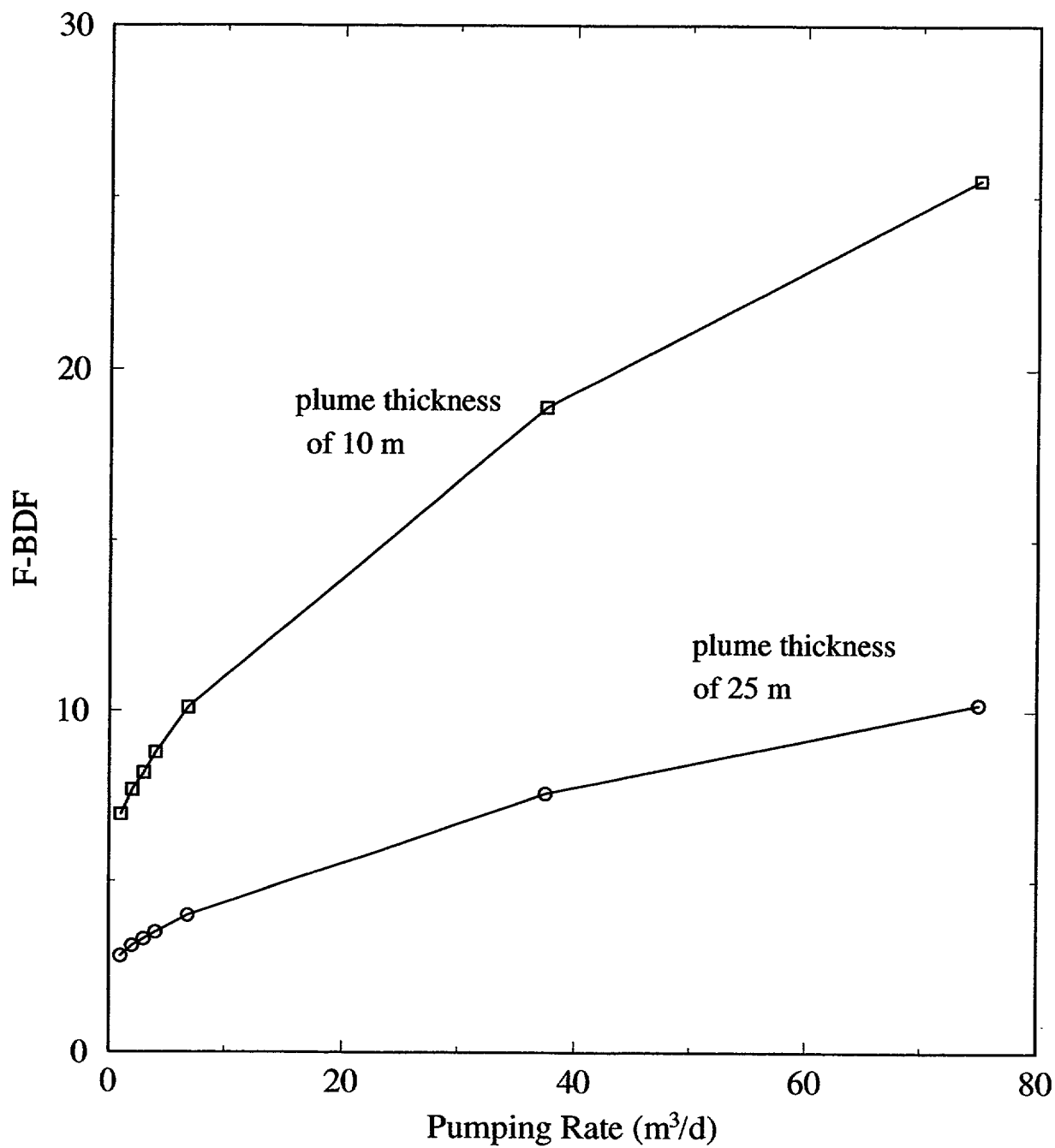


Figure 4-6. Effect of pump rate (range 1 to 75 m³/d) on the flux-based borehole dilution factor for plumes of thickness 10 m and 25 m (no vertical dispersion). The regional gradient is 0.005 and the transmissivity is 100 m²/d for all cases.

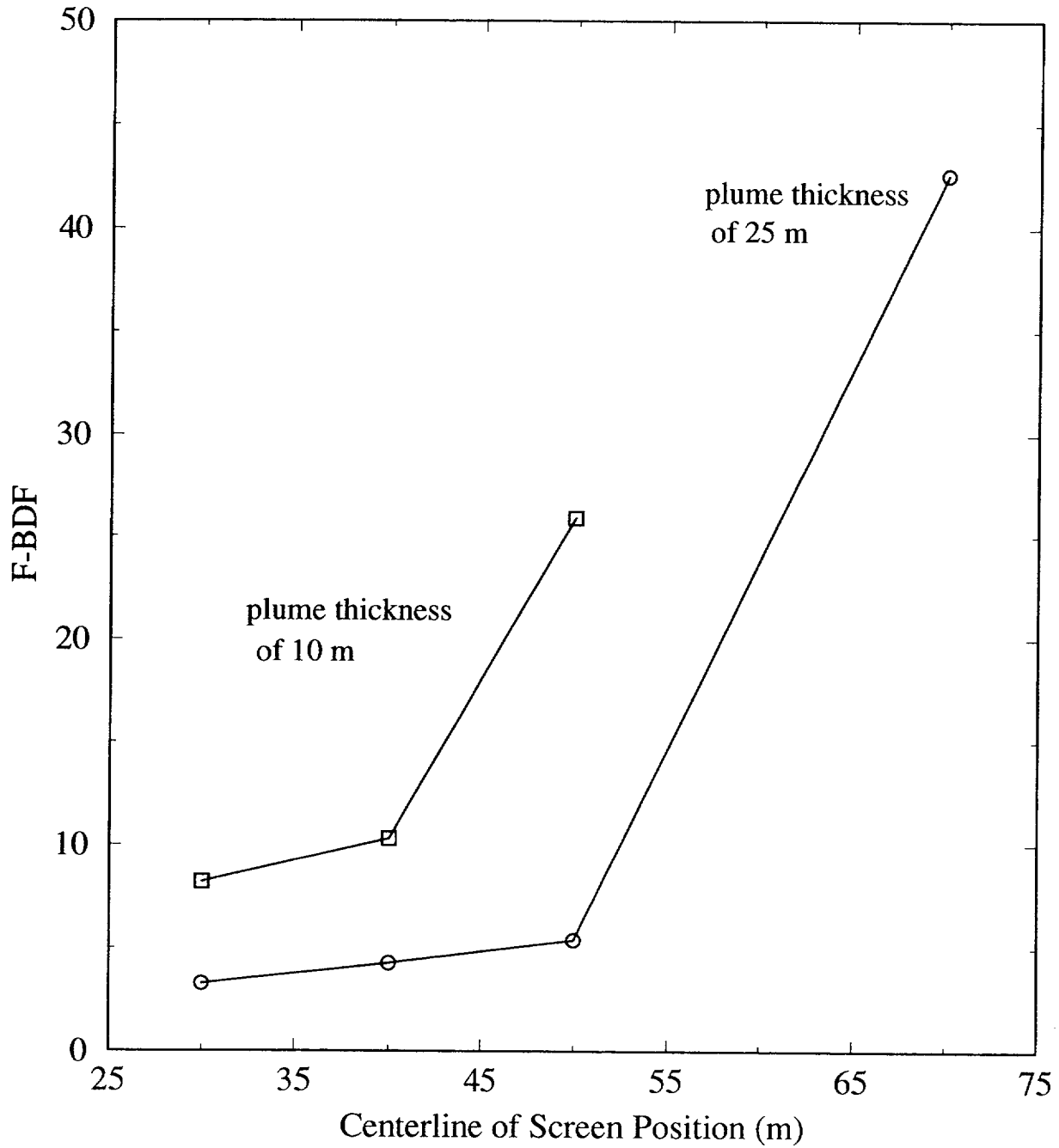


Figure 4-7. Effect of screen position for domestic-sized wells on the flux-based borehole dilution factor for plumes of thickness 10 m and 25 m (no vertical dispersion). All screen lengths are 60 m, the regional gradient is 0.005, and the transmissivity is 100 m²/d for all cases.

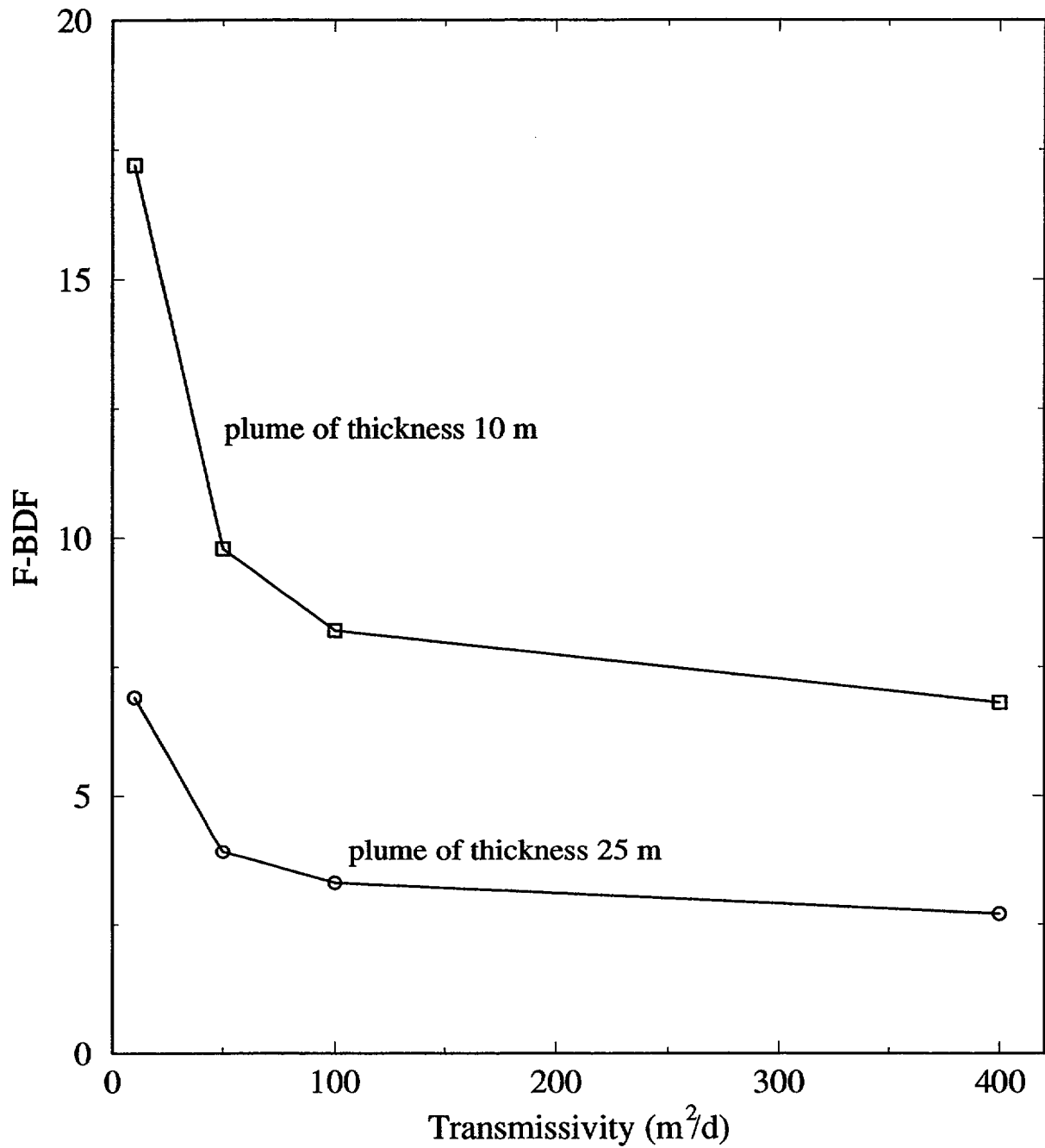


Figure 4-8. Effect of transmissivity (10, 50, 100, 400 m^2/d) on the flux-based borehole dilution factor for plumes of thickness 10 m and 25 m (no vertical dispersion). The regional gradient is 0.005 and the pump rate is 3 m^3/d for all cases.

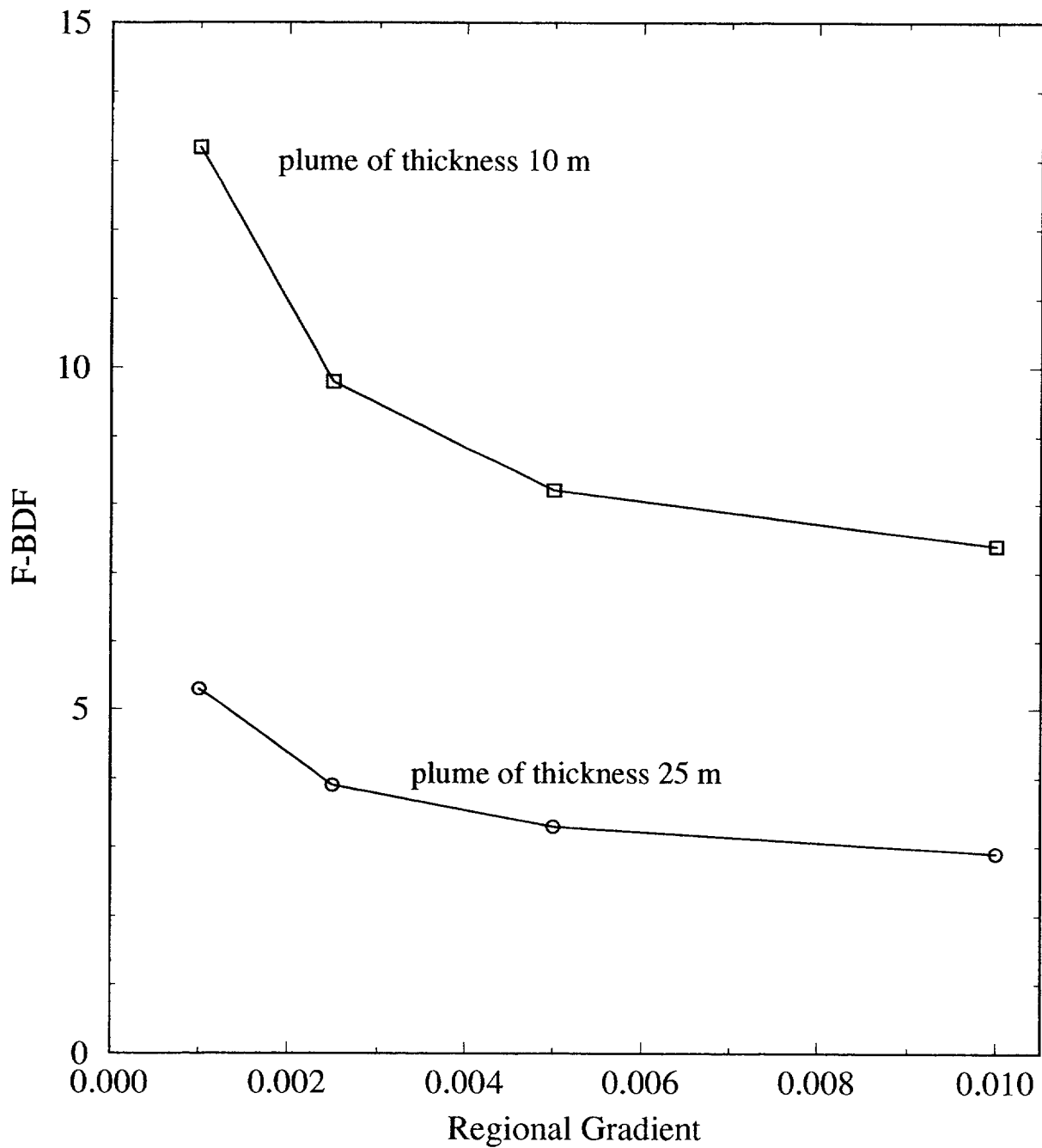


Figure 4-9. Effect of the regional gradient (0.001, 0.0025, 0.005, 0.01) on the flux-based borehole dilution factor for a domestic-sized well and plumes of thickness 10 m and 25 m (no vertical dispersion). The transmissivity is $100 \text{ m}^2/\text{d}$ and the pump rate is $3 \text{ m}^3/\text{d}$ for all cases.

The position of the screened portion of the well does not have a significant effect for domestic wells for the 25-m plume until screened portions are lower than three standard deviations from the average screen position (figure 4-7). The limited effect of screen position is due to a combination of the center of mass of the plume being near the water table as well as the small impact on the capture area due to different screen position and lengths. Within about two standard deviations from the average position of the screen, the F-BDF do not vary by more than a factor of 2. In all scenarios, the plume is assumed to be at the water table. The borehole dilution factors are in the 3 to 5 range and 8 to 10 range for the 25 and 10-m plumes, respectively, unless screen positions lower than three standard deviations from the average are considered.

The effect of transmissivity and regional gradient on F-BDF for the 10 and 25-m-thick plumes with no vertical dispersion are not significant until the smallest values of transmissivity and gradient are used (figures 4-8 and 4-9). For transmissivities greater than $50 \text{ m}^2/\text{d}$, the F-BDF is in the range of 7 to 10 for the 10-m-thick plume and 3 to 7 for the 25-m-thick plume. A regional gradient of 0.001 leads to a F-BDF of 13 for the plume thickness of 10 m while the larger gradients range from 7 to 10. The F-BDF for the 25-m-thick plume are between 3 and 5.

4.3.2 Irrigation Wells and Plumes with No Vertical Dispersion

The F-BDF were calculated for irrigation wells using the scenario of a 25-m-thick plume with no vertical dispersion. In this scenario, the large vertical gradients and deep capture for the wells lead to large amounts of clean water mixing in the borehole with the contaminated water from the plume. Depending on the capture zone width and the plume width, some horizontal mixing of clean and contaminated water may occur. The width of the plume depends on the transverse dispersivity. Figure 4-10 shows the F-BDF for a well pumping rate of 300 to 2,000 m^3/d for plumes using three different dispersivity values. Since the plume width decreases as the dispersivity decreases, the F-BDF increases as the dispersivity decreases. This effect is not present at the low pumping rates for the particular flow field parameters chosen for this comparison. The F-BDF range from 19 to 49 for all dispersivities sets. It must be re-emphasized that the F-BDF only reflects the effects of contaminant concentration reduction in the borehole and not the effects of dispersion on the resident or aquifer contaminant concentrations. This explains the otherwise counter-intuitive observation that, for high capacity wells, the F-BDF increases as the transverse dispersivity decreases.

4.3.3 Irrigation Wells and Plume with Vertical Dispersion

The F-BDF are calculated for irrigation wells using the scenario of a plume where 3D dispersion from a constant concentration source occurs. The effect of dispersion on the concentration during transport on the borehole dilution factor is not considered here; only the shape of the plume is considered in the dilution factors. Generally, the capture zones are thicker and narrower than the thin but wide plumes. Depending on the dispersivity values used for the plume and the pumping rate and hydraulic properties used for the capture zone, the capture zones may be wider than the plume. Only for low pumping rates are the plumes thicker than the capture zone; this occurrence leads to no volumetric-based borehole dilution.

Plume shapes using dispersivities of 100:10:0.1 m and 20:2:0.2 m are compared to capture areas in order to calculate F-BDF. The plume for the 100:10:0.1 scenario is wider but thinner than the plume for the 20:2:0.2 scenario. Figures 4-11 to 4-13 show the effects of pumping rate, transmissivity, and regional gradient on the F-BDF which generally range from 1 to 5 regardless of dispersivity values used. For the pumping rate (figure 4-11) and the regional gradient (figure 4-13) curves, the two

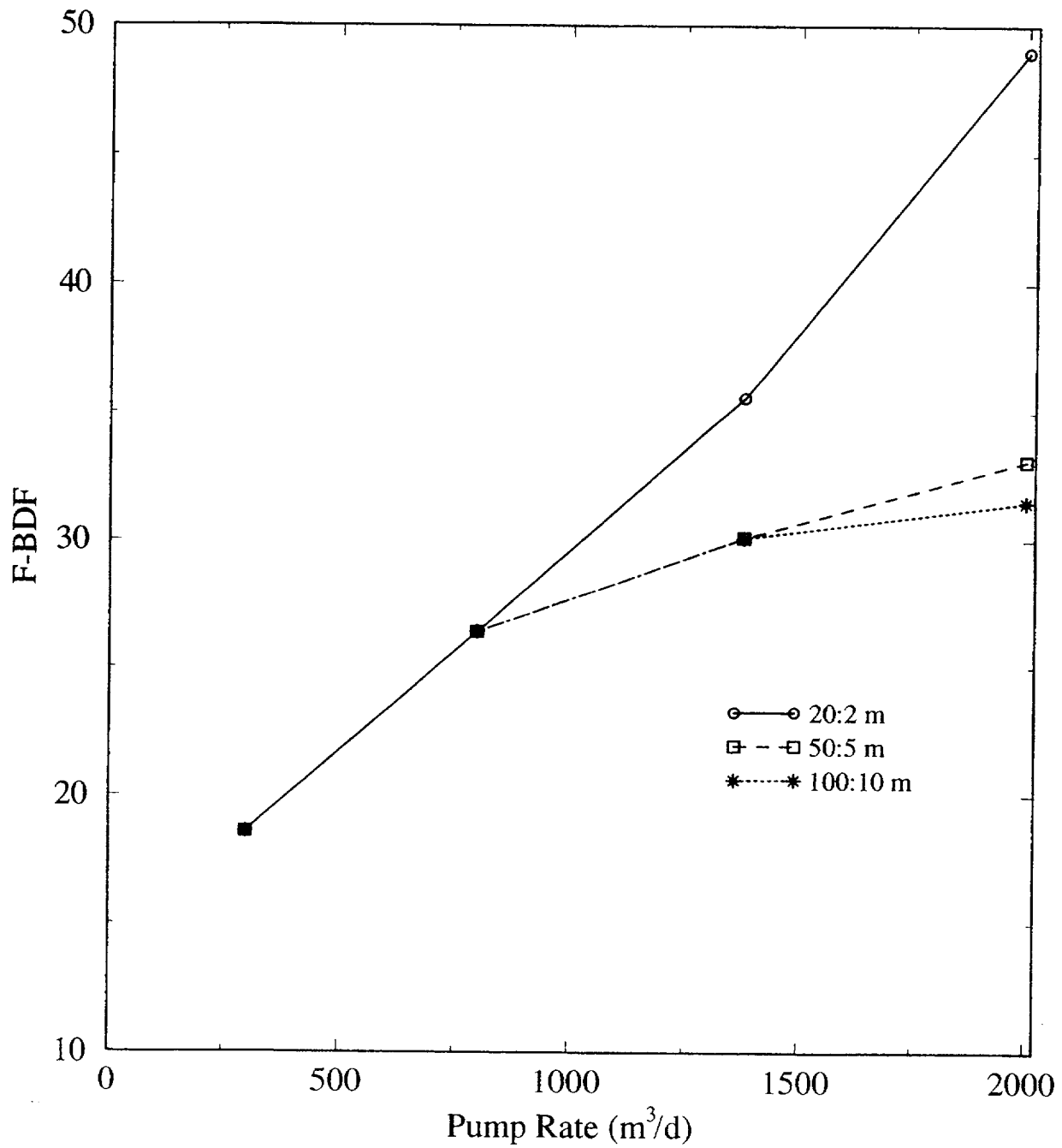


Figure 4-10. Effect of pump rate on flux-based borehole dilution factors for irrigation wells and a 25 m thick plume with no vertical dispersion. Three curves are plotted for different sets of dispersivity values.

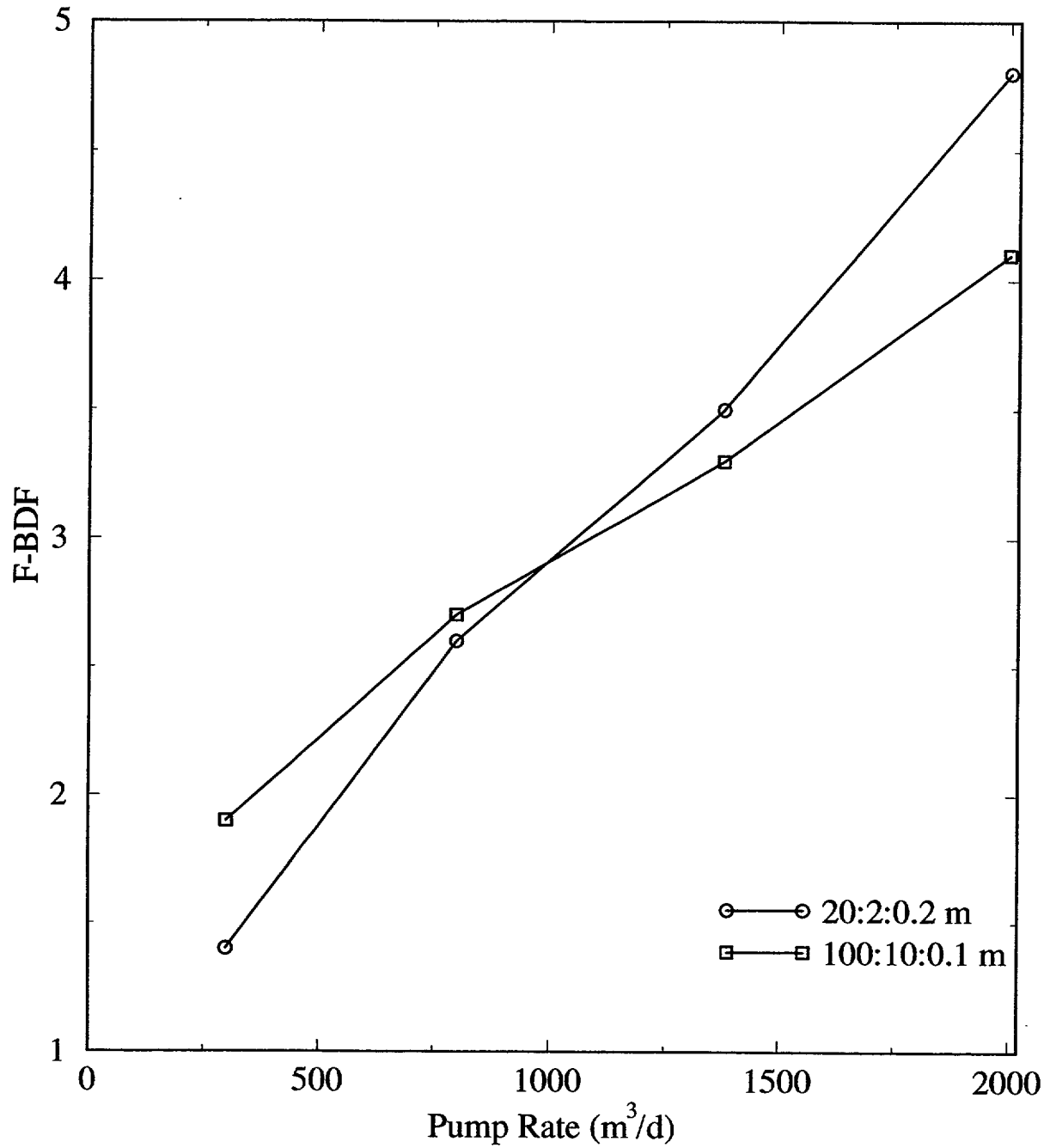


Figure 4-11. Effect of pump rate on dilution factors for irrigation sized wells and a plume with 3D dispersion. Curves are plotted for two sets of dispersivity values.

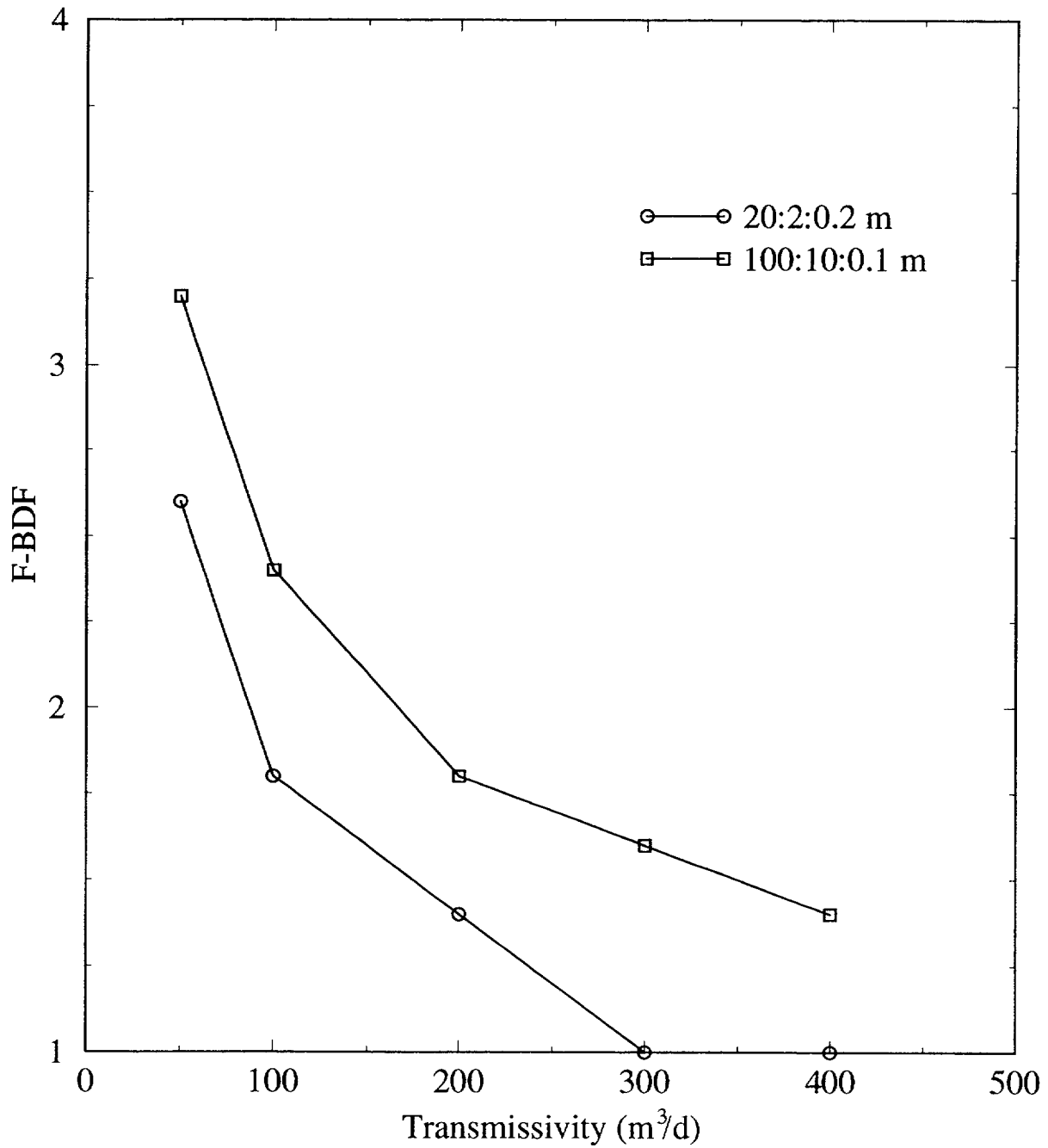


Figure 4-12. Effect of transmissivity (50 to 400 m²/d) on dilution factors for irrigation sized wells and a plume with 3D dispersion. Curves are plotted for two sets of dispersivity values.

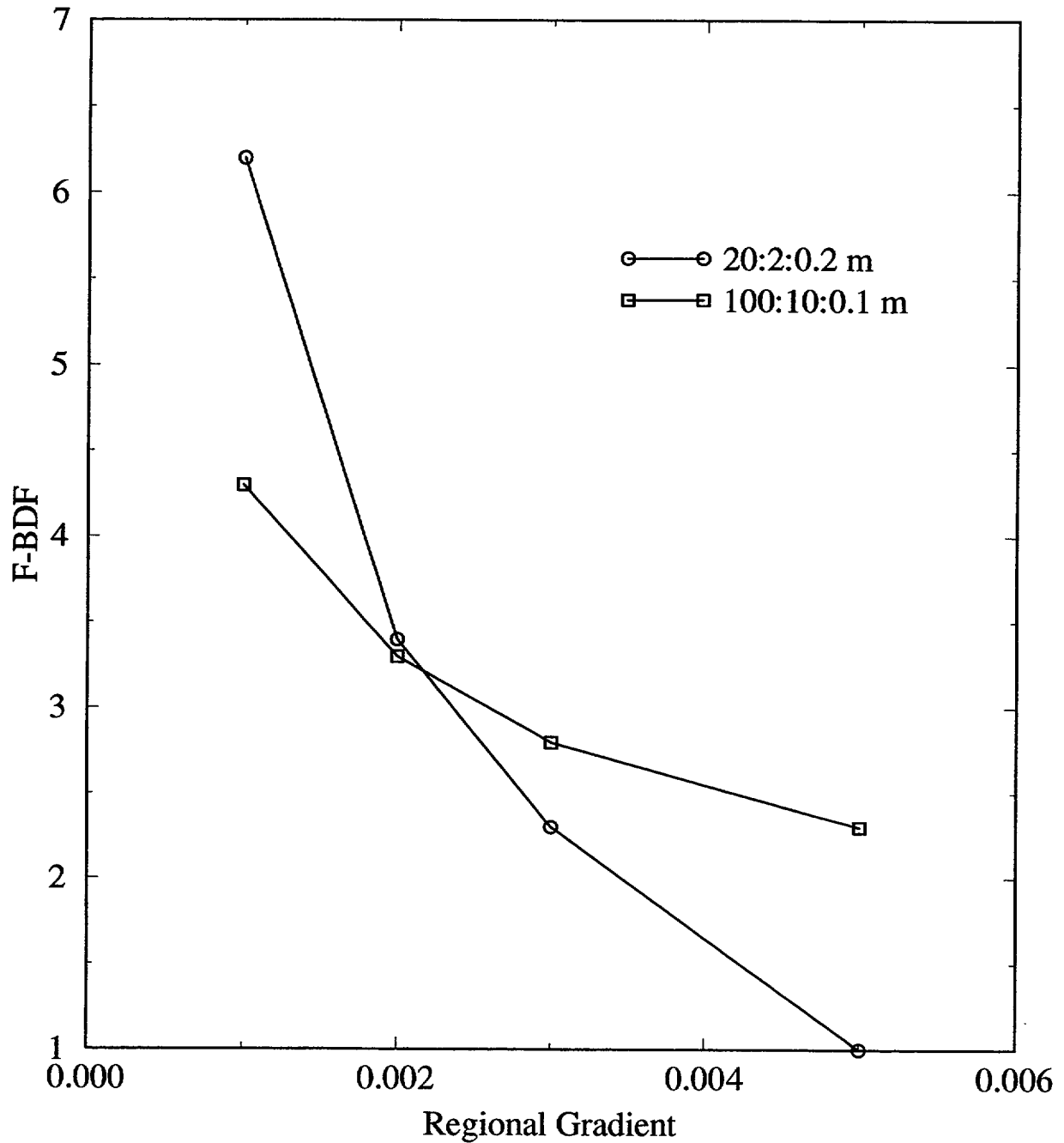


Figure 4-13. Effect of regional hydraulic gradient (0.001 to 0.0005) on dilution factors for irrigation-sized wells and a plume with 3D dispersion. Curves are plotted for two sets of dispersivity values.

dispersivity sets intersect due to the interplay between the thickness of the plume (the 20:2:0.2 plume is thicker) and the point where the entire plume is captured (the 100:10:0.1 plume is larger in area).

In summary, the effect of the plume size has the largest effect on the F-BDF. The values of the dilution factors are tabulated in appendix C. The shapes of plumes described above can be contrasted with the streamtubes used for the TPA (Baca et al., 1997; Manteufel et al., 1997). The plumes increase in size, and volumetric flow rate, with increasing distance from the source. The streamtubes have a fixed thickness and a variable width which depends on the streamlines. The width may increase or decrease for diverging converging, flow fields, respectively, but the volumetric flux does not change.

4.4 BOREHOLE DILUTION FACTORS BASED ON DISPERSIVE TRANSPORT

The F-BDF estimated in the previous section do not account for the concentration distribution of a migrating plume. Kessler and McGuire (1996) accounted for dispersion during plume migration by assuming the dilution factor was the ratio of the source concentration to the centerline concentration. Implicit in their assumption is that the plume has a uniform concentration equal to the centerline value that they justify as a conservative choice in terms of eventual dose to a critical group. This section will address the effect on borehole dilution of a concentration distribution within a plume.

The transport dispersion-based borehole dilution factor (T-BDF) was calculated by integrating the concentration distribution across the area of the portion of the plume which is captured by a pumping well. Portions of the plume not captured by the well do not contribute radionuclide mass to the well. The T-BDF was estimated by numerical integration of the concentration distribution in the area of the plume which was captured. The total borehole dilution factor can be estimated by linear combination of the F-BDF and T-BDF. The effect of domestic and irrigation wells on T-BDF varies significantly due to the thickness of the capture area and will be presented separately.

4.4.1 Domestic Wells

Figures 4-14 and 4-15 illustrate the effect of the concentration distribution within a plume on the T-BDF for two different plume configurations; a thin plume (25-m) with no vertical dispersion and a 3D dispersion plume. The T-BDF for the thin plume is nearly constant and its value is close to that of the P-DF (1.8) for pumping rates in the range of domestic and quasi-municipal wells (figure 4-14). The T-BDF for the plume with 3D dispersion vary from 9 to 18, increasing as the pumping rate increases. The larger values of T-BDF indicate the significance of pumping from less concentrated portions of the plume as compared to the centerline.

T-BDF is inversely proportional to the transmissivity (figure 4-15) with values ranging from 12 to 9 as transmissivity increases. Smaller transmissivity values lead to larger capture areas thus drawing water from portions of the plume with lower concentration. The effect of hydraulic gradient is similar to that of transmissivity.

4.4.2 Irrigation Wells

Figures 4-16 and 4-17 illustrate the effect of the concentration distribution on borehole dilution for irrigation wells. For the plume configuration with 3D dispersion, the T-BDF are as much as five

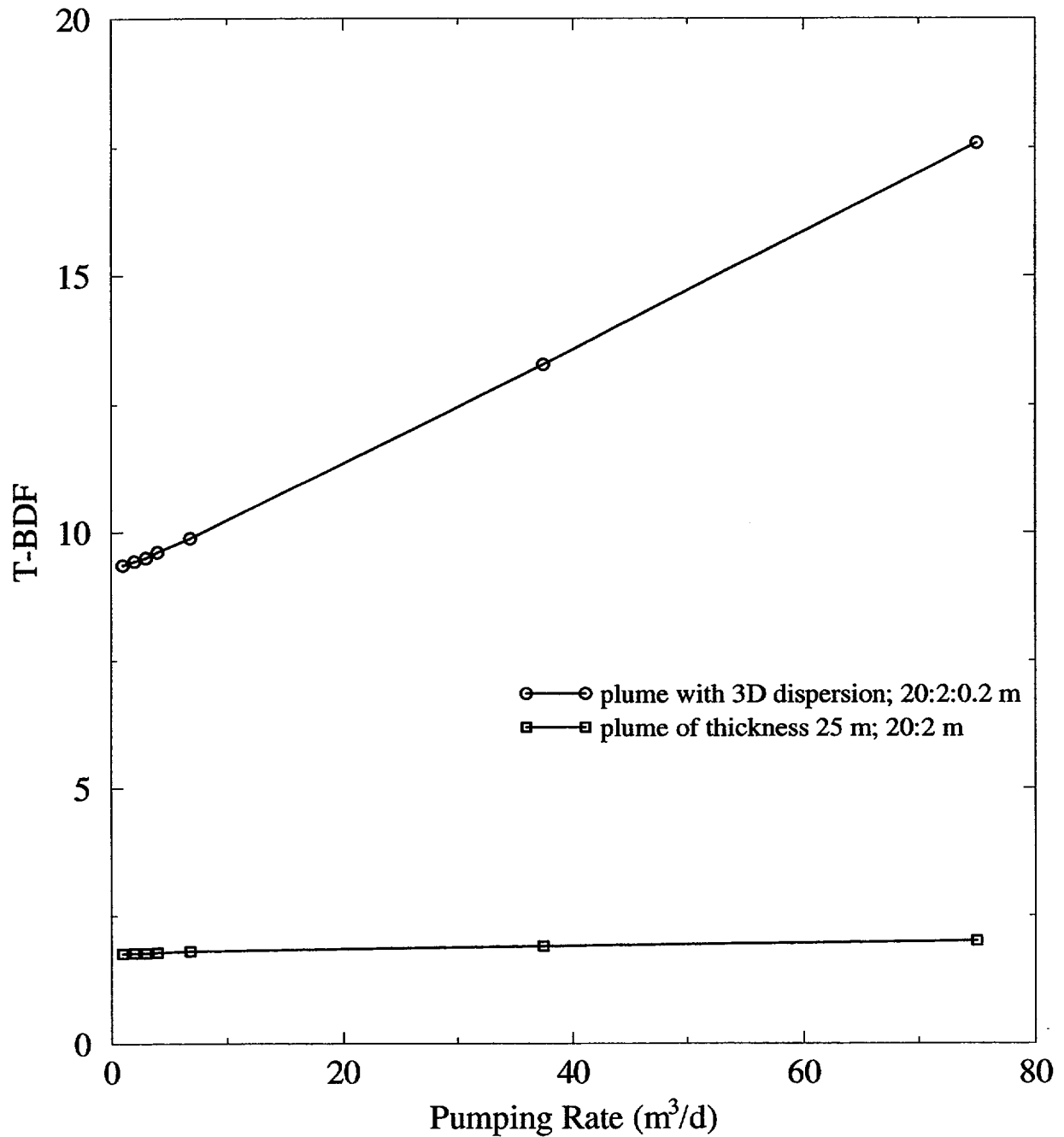


Figure 4-14. Effect of pumping rate (1-75 m³/d) for domestic wells on transport dispersion-based borehole dilution factor for two different plume configurations: a thin plume with no vertical dispersion and a 3D dispersion plume both with dispersivity ratios as noted in the plot

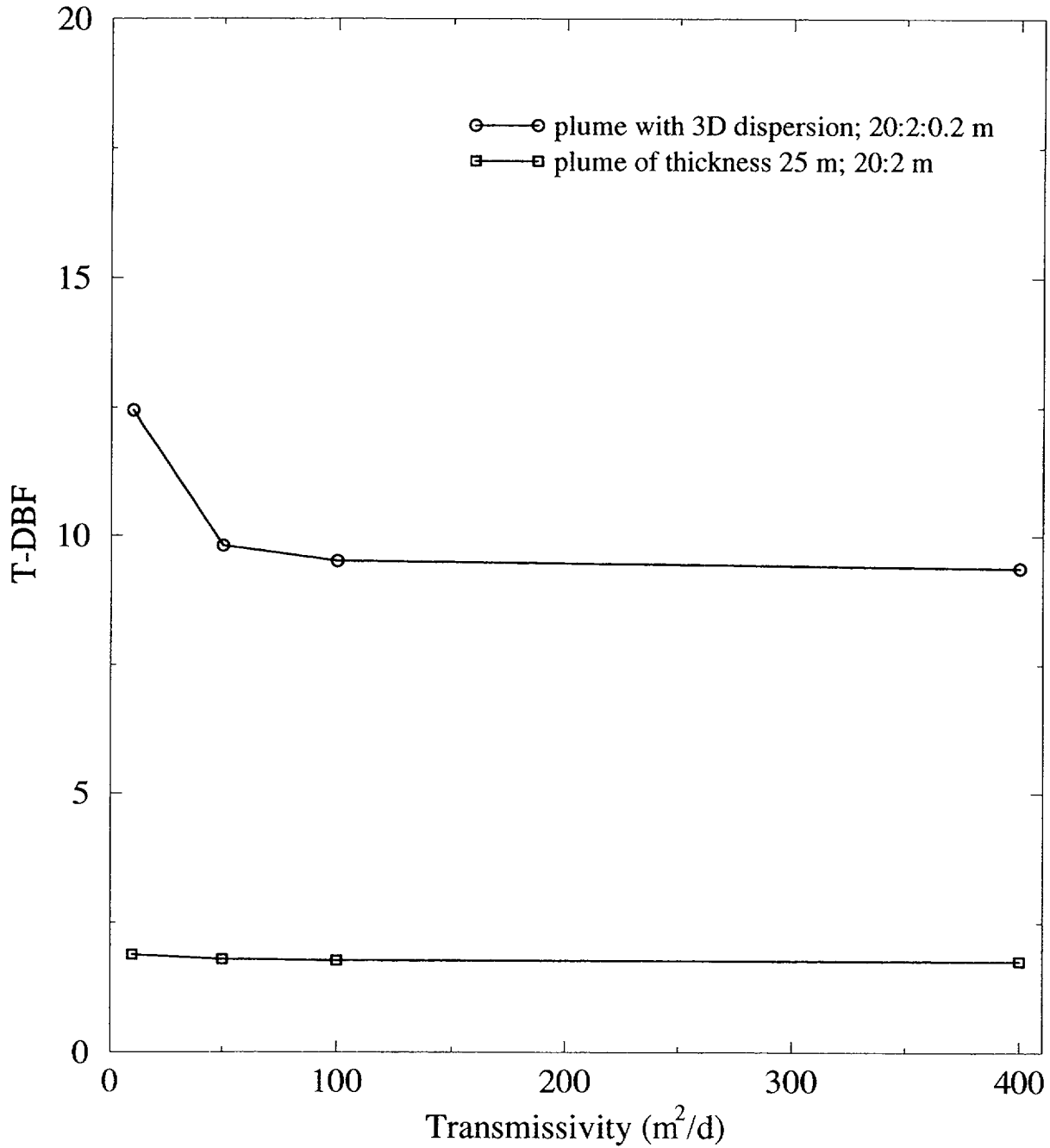


Figure 4-15. Effect of transmissivity (10–400 m²/d) for domestic wells (Q = 3 m³/d) on transport dispersion-based borehole dilution factor for two different plume configurations: a thin plume with no vertical dispersion and a 3D dispersion plume, both with dispersivity ratios as noted in the plot

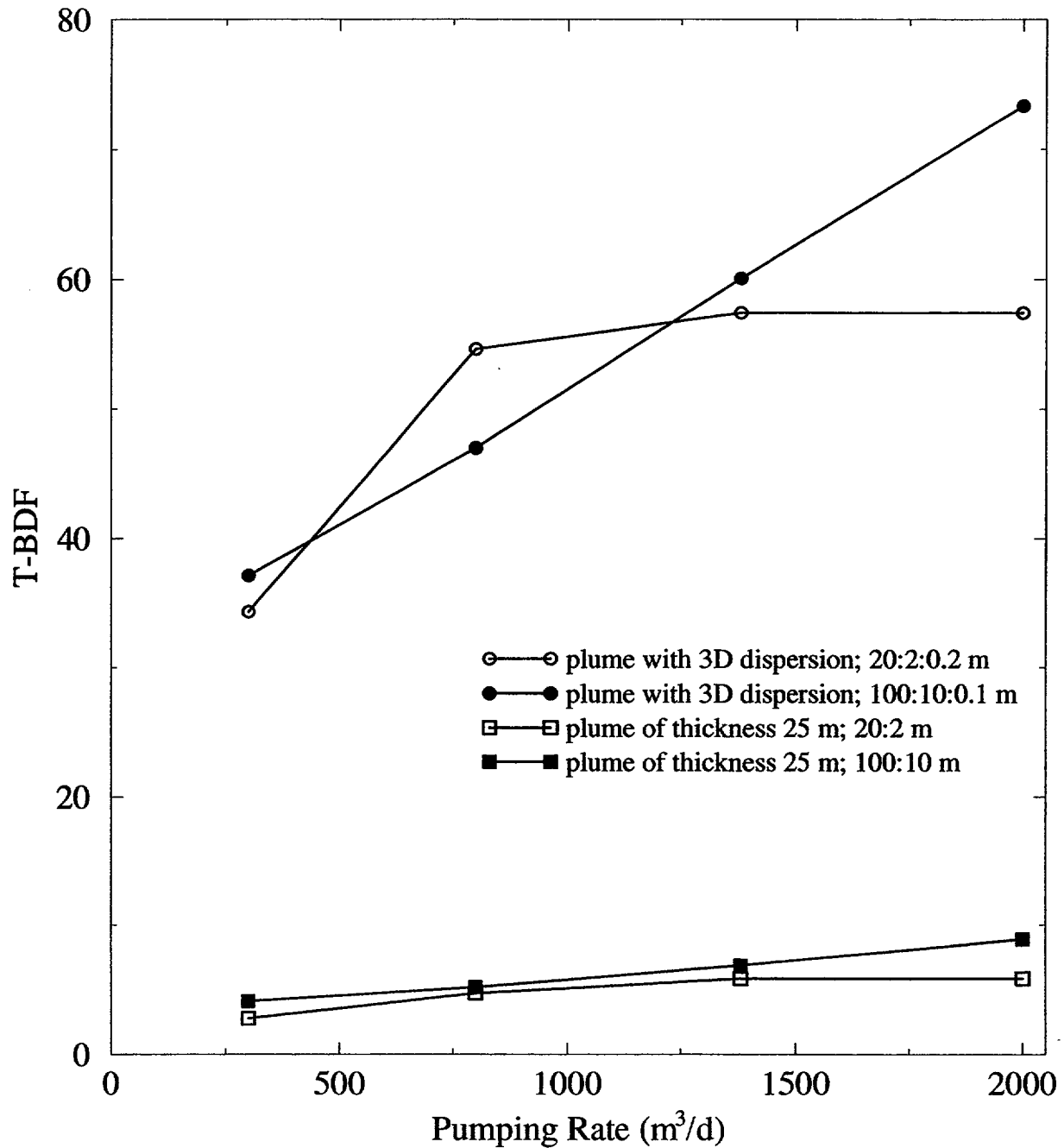


Figure 4-16. Effect of pumping rate (300–2,000 m³/d) for irrigation wells on transport dispersion-based borehole dilution factor for four different plume configurations: two thin plumes with no vertical dispersion and two 3D dispersion plumes, all with dispersivity ratios as noted in the plot

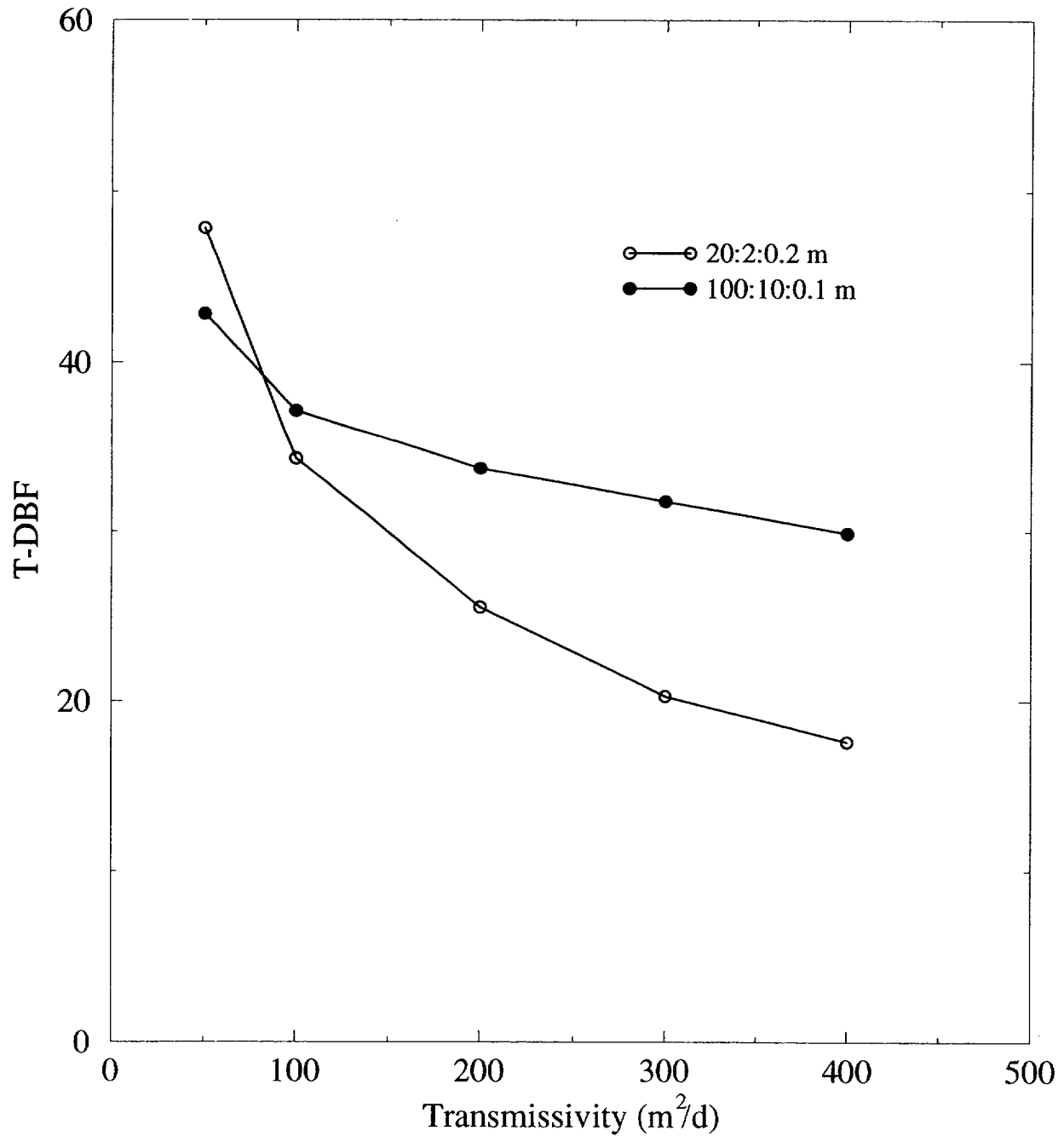


Figure 4-17. Effect of transmissivity (50–400 m²/d) for large irrigation wells (Q=2116 m³/d) on transport dispersion-based borehole dilution factor for two different plume configurations: two 3D dispersion plumes with dispersivity ratios as noted in the plot

times larger (figures 4-14 and 4-16) than those for the domestic wells due to the large thickness of the irrigation capture area drawing in portions of the plume with low concentrations. As with the domestic wells, the T-BDF for thin plumes with no vertical dispersion are near the value of the inverse of the normalized concentration. The straight line increase in T-BDF for the plume with 3D dispersion and dispersivity ratio of 100:10:0.1 m reflects the large size of the plume relative to the capture areas (figure 4-16). The plateau in the curve for the 3D plume with dispersivity ratio of 20:2:0.2 m at the larger pumping rates is due to the entire plume being captured.

For transmissivity increases from 50 to 400 m²/d, the T-BDF decreases from 48 to 18 for the 3D plume with dispersivity ratio of 20:2:0.2 m and from 43 to 30 for the 3D plume with dispersivity ratio of 100:10:0.1 m. Effects due to hydraulic gradient are similar to those of the transmissivity (appendix C).

5 CONCLUSIONS

The approach used in this report to estimate borehole dilution is to separate it into two components: volumetric flux-based and dispersion transport-based components. The method used to estimate F-BDF in the Amargosa Farms region is to compare the capture area of a pumping well to the cross-sectional area of the portion of the plume which is captured. Borehole dilution factors presented in this report are calculated using the cross-sectional areas normal to the principal direction of regional flow. The method used to estimate the component of borehole dilution due to dispersion during transport is to numerically calculate an areal average for the portion of the plume captured by a pumping well. Since this report is a scoping analysis, the F-BDF and T-BDF have been kept separate in order to better delineate sensitive parameters.

Different configurations for the plume and the capture area were evaluated. For domestic wells, the capture area is generally much smaller than the cross-sectional area of a plume that has undergone horizontal and vertical transverse spreading due to macro-dispersion during transport along a 20- to 30-km pathway as shown in figure 4-1. Thus, as expected, F-BDF was minimal when the domestic well was aligned with the center of the plume. Any borehole dilution that might occur would be solely due to vertical gradients in the plume concentration and would be reflected in the T-BDF. For irrigation wells, or any high-discharge wells, the capture area is generally thicker than the plume, while the capture zone may be wider or narrower than the contaminant plume depending on the particular scenario.

To simulate the case in which stratification of the porous medium minimizes the vertical transverse dispersion and thus confines the plume to a thin layer near the water table, a 2D areal advection-dispersion equation was solved for which a fixed plume thickness was assumed. Based on field observations summarized by Gelhar et al. (1992), this non-vertically dispersing plume closely simulates the behavior of many contaminant plumes characterized in the field, and provides a worst-case scenario in terms of high resident concentrations. The position of the plume relative to the capture area affects the dilution factor.

Several conclusions can be drawn from this study. First, as defined in this study, F-BDF for individual wells are relatively small, ranging from 1 to 5 for an irrigation well extracting contaminant from a 3D plume, from 18 to 40 for an irrigation well extracting contaminant from a thin plume that does not disperse vertically, and from 3 to 18 for a domestic well extracting contaminant from a thin plume that does not disperse vertically. However, one must be careful when comparing F-BDF for different contaminant plume configurations since actual borehole concentrations depend on the mass of radionuclides captured and the volume of water pumped, not the area of the plume that is captured. On the one hand, a high-capacity well may capture the entire mass of radionuclides in a large plume, have an apparent dilution factor of only 1, yet still produce a low borehole concentration because the large plume would have a corresponding low mean resident concentration. On the other hand, a low-capacity domestic well may capture the entire mass of radionuclides in a very small plume, have a dilution factor of 10, yet produce a very high borehole concentration because the plume has a very high mean resident concentration.

The T-BDF account for the low or high mean resident concentrations in the different plume scenarios. T-BDF for domestic wells are generally low and approach the P-DF, whereas T-BDF for irrigation wells are up to two orders of magnitude depending on the plume scenario. The P-DF would be a poor estimate for the effect due to dispersion during transport for irrigation wells.

A second, and perhaps obvious, conclusion can be drawn from this study. Specifically, for a thin wide plume of specified dimensions, a low-capacity well screened over a thick section of the aquifer, may produce a higher dilution factor than a larger capacity well screened over a shorter vertical interval. Indeed, extremes in the individual borehole concentrations within a critical group will be greater if the contaminant plume is thin and borehole construction practices are varied, than if the plume is very thick and borehole construction practices are uniform. These results suggest that attention should be paid to understanding vertical spreading in the saturated zone along the presumed transport pathway. Indirect field evidence (Gelhar et al., 1992; Bedient et al., 1994) suggests minimal vertical spreading in alluvial aquifers; however, vertical spreading may be substantial in the fractured tuff aquifer, especially where flow crosses normal faults across which there is significant offset in the conductive and non-conductive strata.

The dilution factors computed in this study cannot be used to estimate borehole concentrations unless the conceptual model of transport adopted by the user conforms to the following description. The solution to the steady state advection-dispersion equation is used to define a material surface that extends from radionuclide source to radionuclide receptor locations through which all radionuclides are transported. The shape of this material surface is best described as a duct or tube bounded on the top by the water table and having a half-elliptical cross-section that increases in area from source to receptor in proportion to the assigned transverse dispersivities. Although radionuclides do not cross the boundary of this tube, water does; the flow rate of water changes in direct proportion to the cross-sectional area of the tube. Hence, under the assumptions of steady state transport, the mean radionuclide concentration computed over the cross-sectional area of the tube at any point along its length must decrease from source to receptor. For the case where vertical transverse dispersion is neglected, the true shape of the tube is not easily described, but the cross-section may be approximated by a vertical rectangle of fixed height whose width increases in direct proportion to the horizontal transverse dispersivity.

The shapes of plumes described above can be contrasted with the streamtubes used in the study by (Baca et al., 1997). The streamtubes have a fixed thickness and a variable width which depends on the streamlines. The width may increase or decrease for diverging or converging flow fields, respectively, but the volumetric flux remains constant within a streamtube.

Further work on borehole dilution would benefit greatly from both a better delineation of a plume entering the Amargosa Farms region and large-scale modeling of multiple-well systems. This report has shown that the plume configuration is an important component. Modeling multiple-well systems is an extension of this work that would better define the pumping effect on groundwater flow patterns in the Amargosa Farms region. The single-well approach used here should only be compared with approaches where the largest volume used for the pumping input is as small as the pumping from a single well. This also assumes that infiltration through the repository or saturated zone mixing beneath the aquifer would both be smaller than the pumping from a single well.

6 REFERENCES

- Akindunni, F.F., W.W. Gillham, B. Conant, Jr., and T. Franz. 1995. Modeling of contaminant movement near pumping wells: Saturated-Unsaturated flow with particle tracking. *Ground Water* 33(2): 264-274.
- Baca, R.G. et al. 1997. *NRC High-Level Radioactive Waste Program Annual Progress Report: Fiscal Year 1996. Chapter 9—Activities Related to Development of The U.S. Environmental Protection Agency Yucca Mountain Standard*. NUREG/CR-6513, No. 1. Washington, DC: U.S. Nuclear Regulatory Commission.
- Bair, E.S., and T.D. Lahm. 1996. Variations in capture-zone geometry of a partially penetrating pumping well in an unconfined aquifer. *Ground Water* 34(5): 842-852.
- Bauer, E.M., and K.D. Cartier. 1995. *Reference Manual for Data Base on Nevada Well Logs*. U.S. Geological Survey Open-File Report 95-460. Washington, DC: U.S. Geological Survey.
- Bedient, P.B., H.S. Rifai, and C.J. Newell. 1994. *Ground Water Contamination Transport and Remediation*. Englewood Cliffs, New Jersey: PTR Prentice Hall.
- Bedinger, M.S., K.A. Sargent, and W.H. Langer. 1989. *Studies of Geology and Hydrology in the Basin and Range Province, Southwestern United States, for Isolation of High-level Radioactive Waste-characterization of the Death Valley Region, Nevada and California*. U.S. Geological Survey Professional Paper 1370-F. Washington, DC: U.S. Geological Survey.
- Buqo, T.S. 1996. *Baseline Water Supply and Demand Evaluation of Southern Nye County, Nevada*. Consultants Report Prepared for the Nye County Nuclear Waste Repository Office, Nye County, Nevada.
- Burchfiel, B.C. 1966. *Reconnaissance Geologic Map of the Lathrop Wells 15-Minute Quadrangle, Nye County, Nevada*. USGS Miscellaneous Geological Investigations Map I-474. Washington, DC: U.S. Geological Survey.
- Chiang, C., G. Raven, and C. Dawson. 1995. The relationship between monitoring well and aquifer solute concentration. *Ground Water* 33(5): 718-726.
- Czarnecki, J.B., and R.K. Waddell. 1984. *Finite-Element Simulations of Groundwater Flow in the Vicinity of Yucca Mountain, Nevada-California*. U.S. Geological Survey Water-Resources Investigations Report 84-4349. Denver, CO: U.S. Geological Survey.
- D'Agnese, F.A. 1994. *Using scientific information systems for three-dimensional modeling of regional ground-water flow systems, Death Valley Region, Nevada and California*. Ph.D. Dissertation, Colorado School of Mines.

- D'Agnese, F.A., C.C. Faunt, A.K. Turner, and M.C. Hill. 1996. *Hydrogeologic Evaluation and Numerical Simulation of the Death Valley Regional Ground-water Flow System, Nevada and California, Using Geoscientific Information Systems*. Washington, DC: U.S. Geological Survey (Draft).
- Denny, C.S., and H. Drewes. 1965. *Geology of the Ash Meadows Quadrangle, Nevada-California*. U.S. Geological Survey Bulletin 1181-L. Washington, DC: U.S. Geological Survey.
- Domenico, P.A., and G.A. Robbins. 1985. A new method of contaminant plume analysis. *Ground Water* 23(4): 476-485.
- Fabryka-Martin, J.F., P.R. Dixon, S. Levy, B. Liu, H.J. Turin, and A.V. Wolfsberg. 1996. *Summary Report of Chlorine-36 Studies: Systematic Sampling for Chlorine-36 in the Exploratory Studies Facility*. LA-UR-96-1384. Los Alamos, NM: Los Alamos National Laboratory.
- Faybishenko, B.A., I. Javandel, and P.A. Witherspoon. 1995. Hydrodynamics of the capture zone of a partially penetrating well in a confined aquifer. *Water Resources Research* 31(4): 859-866.
- Fischer, J.M. 1992. *Sediment properties and water movement through shallow unsaturated alluvium at an arid site for disposal of low-level radioactive waste near Beatty, Nye County, Nevada*. U.S. Geological Survey Water-Resources Investigations Report 92-4032. Washington, DC: U.S. Geological Survey.
- Flint, A.L., and L.E. Flint. 1994. Spatial distribution of potential near surface moisture flux at Yucca Mountain. *High-Level Radioactive Waste Management: Proceedings of the Fifth International Conference, Las Vegas, Nevada, May 22-26, 1994*. La Grange Park, IL: American Nuclear Society: 2352-2358.
- Gelhar, L.W., C. Welty, and K.R. Rehfeldt. 1992. A critical review of data on field-scale dispersion in aquifers. *Water Resources Research* 28(7): 1,955-1,974.
- Grubb, S. 1993. Analytical model for estimation of steady-state capture zones of pumping wells in confined and unconfined aquifers. *Ground Water* 31(1): 27-32.
- Haitjema, H.M. 1995. *Analytic Element Modeling of Groundwater Flow*. New York: Academic Press.
- Hoover, D.L., W.C. Swadley, and A.J. Gordon. 1981. *Correlation Characteristics of Surficial Deposits With a Description of Surficial Stratigraphy in the Nevada Test Site Region*; USGS. Open-File Report 81-512. Washington, DC: U.S. Geological Survey.
- Kessler, J., and R. McGuire. 1996. *Yucca Mountain Total System Performance Assessment, Phase 3*. EPRI TR-107191. Palo Alto, CA: Electric Power Research Institute.
- Kilroy, K.C. 1991. *Ground-Water Conditions in Amargosa Desert, Nevada-California, 1952-87*. U.S. Geological Survey Water-Resources Investigations Report 89-4101. Washington, DC: U.S. Geological Survey.

- Laczniak, R.J., J.C. Cole, D.A. Sawyer, and D.A. Trudeau. 1996. *Summary of Hydrologic Controls on Ground-Water Flow at the Nevada Test Site, Nye County, Nevada*. U.S. Geological Survey Water-Resources Investigations Report 96-4109. Washington, DC: U.S. Geological Survey.
- Manteufel, R.D., R.G. Baca, S. Mohanty, M.S. Jarzempa, R.W. Janetzke, S.A. Stothoff, C.B. Connor, G.A. Cragnolino, A.H. Chowdhury, T.J. McCartin, and T.M. Ahn. 1997. *Total-system Performance Assessment (TPA) Version 3.0 Code: Module Descriptions and User's Guide*. San Antonio, TX: Center for Nuclear Waste Regulatory Analyses.
- Mohanty, S., G.A. Cragnolino, T. Ahn, D.S. Dunn, P.C. Lichtner, R.D. Manteufel, N. Sridhar. 1997. *Engineered Barrier System Performance Assessment Code: EBSPAC Version 1.1: Technical Description and User's Manual*. San Antonio, TX: Center for Nuclear Waste Regulatory Analyses.
- Naff, R.L. 1973. *Hydrogeology of the southern part of the Amargosa Desert in Nevada*. Master's Thesis: University of Nevada at Reno.
- Nevada Division of Water Resources. 1997a. *Well Driller's Logs for Amargosa Desert Townships 15, 16, 17S and Ranges 47, 48, 49, 50E from Nevada Division of Water Resources*. Carson City, NV: Nevada Division of Water Resources.
- Nevada Division of Water Resources. 1997b. *Annual Estimates of Water Use for Hydrographic Basin 230, Amargosa Desert*. Carson City, NV: Nevada Division of Water Resources.
- Nevada Division of Water Resources. 1997c. *Well Permit Database for Hydrographic Basin 230, Amargosa Desert*. Carson City, NV: Nevada Division of Water Resources.
- Nichols, W.D., and J.P. Akers. 1985. *Water-Level Declines in the Amargosa Valley area, Nye County, Nevada, 1962-84*. U.S.G.S. Water-Resources Investigations Report 85-4273. Washington, DC: U.S. Geological Survey.
- Nuclear Regulatory Commission. 1995. *NRC Iterative Performance Assessment Phase 2: Development of Capabilities for Review of a Performance Assessment for a High-Level Waste Repository*. NUREG-1464. Washington, DC: Nuclear Regulatory Commission.
- Oatfield, W.J., and J.B. Czarnecki. 1991. Hydrogeologic inferences from drillers' logs and from gravity and resistivity surveys in the Amargosa Desert, southern Nevada. *Journal of Hydrology* 124: 131-158.
- Osterkamp, W.R., L.J. Lane, and C.S. Savard. 1994. Recharge estimates using a geomorphic/distributed-parameter simulation approach, Amargosa River Basin. *Water Resources Bulletin* 30(3): 493-507.
- Plume, R.W. 1996. *Hydrogeologic Framework of the Great Basin Region of Nevada, Utah, and Adjacent States*. U.S. Geological Survey Professional Paper 1409-B. Washington, DC: U.S. Geological Survey.

- Reilly, T.E., O.L. Franke, and G.D. Bennett. 1989. Bias in groundwater samples caused by wellbore flow. *Journal of Hydraulic Engineering* 115(2): 270-276.
- Savard, C.S. 1995. *Selected Hydrologic Data from Fortymile Wash in the Yucca Mountain Area, Nevada, Water Year 1992*. U.S. Geological Survey Open-File Report 94-317. Washington, DC: U.S. Geological Survey.
- Schafer, D.C. 1996. Determining 3D capture zones in homogeneous, anisotropic aquifers. *Ground Water* 34(4): 628-639.
- Stothoff, S.A. 1997. Sensitivity of long-term bare soil infiltration simulations to hydraulic properties in an arid environment. *Water Resources Research* 33(4): 547-558.
- Strack, O.D.L. 1989. *Groundwater Mechanics*. Englewood Cliffs, NJ: Prentice-Hall.
- Swadley, W.C. 1983. *Map Showing Surficial Geology of the Lathrop Wells Quadrangle, Nye County, Nevada*. USGS Misc. Invest. Series I-1361. Washington, DC: U.S. Geological Survey.
- Swadley, W.C., and W.J. Carr. 1980. *Geologic Map of the Quaternary and Tertiary deposits of the Big Dune Quadrangle, Nye County, Nevada, and Inyo County, California*. USGS Misc. Invest. Series I-1361. Washington, DC: U.S. Geological Survey.
- TRW Environmental Safety Systems, Inc. 1995. *Total System Performance Assessment-1995: An Evaluation of the Potential Yucca Mountain Repository*. B00000000-01717-2200-00136. Las Vegas, NV: TRW Environmental Safety Systems, Inc.
- U.S. Department of Energy. 1988. *Site Characterization Plan: Yucca Mountain Site, Nevada Research and Development Area, Nevada, Volume II, Part A*. Oak Ridge, TN: U.S. Department of Energy, Office of Civilian Radioactive Management.
- U.S. Geological Survey. 1989. *National Water Information System User's Manual Volume 2, Chapter 4. Ground-Water Site Inventory System*. U.S. Geological Survey Open-File Report 89-587. Washington, DC: U.S. Geological Survey.
- Walker, G.E., and T.E. Eakin. 1963. *Geology and Ground Water of Amargosa Desert, Nevada-California*. Nevada Department of Conservation and Natural Resources, Ground-Water Resources-Reconnaissance Series Report 14. Carson City, NV: Nevada Department of Conservation and Natural Resources.
- Wexler, E.J. 1992. Analytical solutions for one-, two-, and three-dimensional solute transport in ground-water systems with uniform flow. *Techniques of Water-Resources Investigations of the U.S. Geological Survey*, Chapter B7, Book 3 of Applications of Hydraulics. Washington, DC: U.S. Geological Survey.

Wilson, M.L., J.H. Gauthier, R.W. Barnard, G.E. Barr, H.A. Dockery, E. Dunn, R.R. Eaton, D.C. Guerin, N. Lu, M.J. Martinez, R. Nilson, C.A. Rautman, T.H. Robey, B. Ross, E.E. Ryder, A.R. Schenker, S.A. Shannon, L.H. Skinner, W.G. Halsey, J.D. Gansemer, L.C. Lewis, A.D. Lamont, I.R. Triay, A. Meijer, and D.E. Morris. 1994. *Total-System Performance Assessment for Yucca Mountain - SNL Second Iteration (TSPA-1993) - Volume 1*, Sandia Report SAND93-2675. Albuquerque, NM: Sandia National Laboratories.

Winograd, I.J., and W. Thordarson. 1975. *Hydrogeologic and Hydrochemical Framework, South-Central Great Basin, Nevada-California, with Special Reference to the Nevada Test Site*. U.S. Geological Survey Professional Paper 712-C. Washington, DC: U.S. Geological Survey.

APPENDIX A

DETAILED WATER USE TABLES FOR 1983, 1985-1996

Table A-1. Annual water use estimates (acre-ft) from NDWR (1997b); qq = quarter-quarter section, qtr = quarter section, sec = section, twm = township, rng = range, xx = not recorded, com = commercial, mm = mining, irr = irrigation, qm = quasi-municipal

qq qtr sec twm rng	Use	1996	1995	1994	1993	1992	1991	1990	1989	1988	1987	1986	1985	1983
se se 13 15 49	com	0.5	—	—	—	—	—	—	—	—	—	—	—	—
se ne 16 16 48	com	2	—	—	—	—	—	—	—	—	—	—	—	—
ne ne 14 16 49	com	0.1	—	—	—	—	—	—	—	—	—	—	—	—
ne nw 12 17 48	mm	272	349	340	232	347.5	335	383	525	569	298	284	110	255
ne nw 25 18 50	com	—	—	—	—	—	—	—	—	0.5	0.5	0.6	—	—
xx se 35 16 49	com	1.0	—	—	—	—	—	—	—	—	—	—	—	—
xx sw 36 17 49	com	746.5	431	377	512	306	115	503.1	888	427	4	266	840	—
nw ne 10 17 49	com	50	—	—	—	—	—	—	—	—	—	—	—	—
ne nw 10 16 48	irr	—	300	60	—	—	—	—	—	385	385	385	375	400
ne nw 8 16 48	irr	—	—	—	—	—	—	—	—	—	—	—	—	150
ne ne 16 16 48	irr	125	400	280	290	600	400	400	50	700	100	600	400	—
sw nw 7 16 48	irr	92.5	185	185	185	37	37	—	—	—	—	—	—	—
xx xx 36 16 48	irr	799.5	864.5	1,170	1,170	994.5	1170	25	—	—	860	864.5	864.5	625
nw nw 18 16 48	irr	400	400	480	200	—	—	—	—	200	—	600	300	—
ne se 14 16 48	irr	175	175	175	175	—	—	—	—	—	—	—	—	—
ne ne 23 16 48	irr	625	625	625	668.8	625	800	—	—	—	—	—	325	625
ne sw 25 16 48	irr	—	—	—	—	625	—	—	—	—	—	—	625	625
nw ne 17 16 48	irr	—	—	50	—	—	—	—	—	—	—	—	128.9	75
ne nw 15 16 48	irr	5	12.5	15	2	2	—	10	—	—	—	—	—	—
ne nw 15 16 48	irr	7.5	2.5	2.5	1	4	—	—	—	6.3	—	—	—	—
ne ne 8 16 48	irr	5	90	75	90	—	—	—	—	50	—	195	—	—
sw nw 20 16 48	irr	17.5	17.5	10	20	40	20	—	—	—	—	—	—	300

A-1

Table A-1. Annual water use estimates (acre-ft) from NDWR (1997b); qq = quarter-quarter section, qtr = quarter section, sec = section, twn = township, rng = range, xx = not recorded, com = commercial, mm = mining, irr = irrigation, qm = quasi-municipal (cont'd)

qq qtr sec twn rng	Use	1996	1995	1994	1993	1992	1991	1990	1989	1988	1987	1986	1985	1983
ne ne 24 16 48	irr	227.5	300	200	175	175	175	150	175	175	175	—	—	—
ne se 24 16 48	irr	625	625	625	—	200	200	—	—	—	—	—	—	—
ne ne 36 16 48	irr	25	50	50	190	16	—	25	25	—	—	—	—	—
se sw 10 16 48	irr	—	400	—	200	—	—	—	—	—	—	—	—	—
se nw 18 16 48	irr	657.5	683	540.8	328.5	—	—	—	—	47.2	—	777.25	656.25	—
se sw 10 16 48	irr	5	5	—	—	—	—	—	—	—	—	—	—	—
nw sw 10 16 48	irr	17.5	17.5	17.5	17.5	17.5	—	5	5	2.5	2.5	2.5	—	—
nw sw 10 16 48	irr	11.25	—	—	—	—	—	—	—	—	—	—	—	—
nw sw 10 16 48	irr	—	—	—	—	1	—	22.5	—	—	—	—	—	—
sw se 8 16	irr	24	99	99	54	—	—	—	—	5	—	—	—	60
nw nw 15 16 48	irr	12.5	10	10	2	6	—	—	—	—	—	—	—	20
se nw 26 16 481	irr	583.5	583.5	223.34	250	—	—	250	—	—	583.5	583.5	583.5	584
se ne 26 16 48	irr	233.4	233.4	—	—	—	—	583.5	—	—	583.5	583.5	583.5	584
sw se 8 16 48	irr	70.7	75	60	30	—	—	—	—	—	—	—	—	—
sw nw 24 16 48	irr	583.5	583.5	583.5	583.4	—	—	583.35	—	—	583.35	538.35	583.35	—
sw nw 15 16 48	irr	10	10	20.65	6	6	—	—	—	34.4	—	—	25	—
nw nw 15 16 48	irr	12.5	—	—	—	—	—	—	—	—	—	—	—	—
ne nw 15 16 48	irr	5	—	—	—	—	—	—	—	—	—	—	—	—
ne nw 15 16 48	irr	1	—	—	—	—	—	—	—	—	—	—	—	—
nw nw 15 16 48	irr	5	—	—	—	—	—	—	—	—	—	—	—	—
ne nw 15 16 48	irr	1	—	—	—	—	—	—	—	—	—	—	—	—

A-2

Table A-1. Annual water use estimates (acre-ft) from NDWR (1997b); qq = quarter-quarter section, qtr = quarter section, sec = section, twm = township, rng = range, xx = not recorded, com = commercial, mm = mining, irr = irrigation, qm = quasi-municipal (cont'd)

qq qtr sec twm rng	Use	1996	1995	1994	1993	1992	1991	1990	1989	1988	1987	1986	1985	1983
ne ne 28 16 49	irr	183.4	183.4	183.4	183.4	183.4	—	75	75	183.4	183.4	183.4	109.9	210
ne sw 9 16 49	irr	—	—	—	—	—	—	—	—	—	—	—	—	5
ne se 32 16 49	irr	—	—	—	—	—	—	139.5	—	—	—	—	—	—
ne ne 14 16 49	irr	—	—	—	55	55	—	—	—	—	—	—	—	—
ne nw 30 16 49	irr	665	665	665	665	—	—	677.5	—	—	266	—	—	—
ne nw 35 16 49	irr	—	—	—	2	2	—	—	—	—	—	—	—	—
ne se 19 16 49	irr	625	625	625	625	625	625	400	250	—	—	—	—	—
se sw 9 16 49	irr	105	118.75	50	118.3	118.75	—	118.75	118.8	75	75	75	50	118.8
ne ne 8 16 49	irr	27.5	90	15	10	10	—	25	25	—	—	—	—	98.5
sw se 5 16 49	irr	—	—	1	—	—	—	—	—	—	—	—	—	—
ne se 8 16 49	irr	5	2	—	4	4	—	—	—	—	—	—	—	—
se nw 35 16 49	irr	26.28	26.2	18.2	18.2	18.24	—	—	—	—	—	—	—	—
se sw 9 16 49	irr	25	25	25	25	25	25	25	25	25	25	25	25	25
ne se 23 16 49	irr	625	625	625	625	625	625	—	—	—	—	—	—	625
nw ne 8 16 49	irr	—	—	—	13.7	—	—	—	—	—	—	—	—	—
se sw 9 16 49	irr	25	25	25	25	25	25	25	—	25	25	25	25	25
se se 22 16 49	irr	5	—	35	47.7	—	—	15	15	10	10	—	22.7	—
se ne 12 17 48	irr	—	—	—	—	—	—	—	—	—	—	—	—	25
se nw 12 17 48	irr	65	65	65	65	65	65	65	65	45	45	45	75	—
ne nw 9 17 49	irr	—	—	—	690	540	550	790	400	300	200	—	—	—
ne ne 9 17 49	irr	700	700	700	—	—	—	—	—	—	—	—	—	—

Table A-1. Annual water use estimates (acre-ft) from NDWR (1997b); qq = quarter-quarter section, qtr = quarter section, sec = section, twm = township, rng = range, xx = not recorded, com = commercial, mm = mining, irr = irrigation, qm = quasi-municipal (cont'd)

qq qtr sec twm rng	Use	1996	1995	1994	1993	1992	1991	1990	1989	1988	1987	1986	1985	1983
ne nw 15 17 49	irr	25	25	20	16	16	—	12	12	12	12	—	25	—
se se 8 17 49	irr	—	118.5	—	—	—	—	181.1	—	—	—	—	—	—
ne ne 9 17 49	irr	170	170	—	—	—	—	—	—	—	—	—	—	—
ne ne 9 17 49	irr	628	628	312.5	628	—	—	—	—	—	—	—	—	—
xx sw 4 16 48	irr	—	—	—	—	—	—	—	—	375	—	—	—	—
xx nw 23 16 48	irr	—	—	—	—	—	—	—	—	—	—	—	—	625
xx nw 25 16 48	irr	—	—	—	—	—	—	—	—	—	—	—	—	625
nw nw 15 16 48	irr	7.5	—	—	—	—	—	—	—	—	—	—	—	—
xx nw 25 16 48	irr	625	625	625	—	—	—	—	—	—	—	—	625	—
xx nw 25 16 48	irr	625	625	—	—	—	—	—	—	—	—	—	—	—
ne nw 17 16 48	irr	—	60	60	—	—	—	—	—	—	—	—	240	—
sw se 32 16 49	irr	—	—	100	100	—	175	175	175	—	—	—	—	—
ne ne 28 16 49	irr	—	—	—	—	—	—	—	—	—	—	—	100	—
nw se 1 17 48	irr	—	—	—	—	—	—	—	—	—	—	—	—	625
se nw 12 17 48	irr	—	—	—	—	—	—	—	—	—	—	—	—	300
ne se 12 17 48	irr	50	50	50	50	50	50	125	125	—	—	—	—	—
xx se 1 17 48	irr	40	40	—	—	—	—	—	—	—	375	375	375	—
sw ne 9 17 49	irr	40	40	—	—	—	—	—	—	—	—	—	—	—
se ne 9 17 49	irr	40	40	—	—	—	—	—	—	—	—	—	—	—
xx se 7 17 49	irr	—	—	—	—	—	—	—	—	—	200	—	625	—
xx sw 7 17 49	irr	625	625	—	—	—	—	50	—	312.5	625	625	25	—

A-4

Table A-1. Annual water use estimates (acre-ft) from NDWR (1997b); qq = quarter-quarter section, qtr = quarter section, sec = section, twn = township, rng = range, xx = not recorded, com = commercial, mm = mining, irr = irrigation, qm = quasi-municipal (cont'd)

qq qtr sec twn rng	Use	1996	1995	1994	1993	1992	1991	1990	1989	1988	1987	1986	1985	1983
ne sw 9 17 49	irr	200	200	00	—	—	—	—	—	—	—	—	—	—
nw sw 9 17 49	irr	200	200	50	—	—	—	—	—	—	—	—	—	—
nw se 7 17 49	irr	—	—	—	—	—	—	—	—	—	—	—	—	625
nw sw 7 17 49	irr	—	—	—	—	—	—	—	—	—	—	—	—	312.5
nw ne 24 15 49	qm	8	—	—	—	—	—	—	—	—	—	—	—	—
ne nw 27 16 49	qm	3.4	—	—	—	—	—	—	—	—	—	—	—	—
sw se 31 16 49	qm	10.5	—	—	—	—	—	—	—	—	—	—	—	—
se se 26 16 49	qm	0.1	—	—	—	—	—	—	—	—	—	—	—	—
nw ne 16 16 49	qm	20	—	—	—	—	—	—	—	—	—	—	—	—
se sw 1 17 48	qm	7.5	—	—	—	—	—	—	—	—	—	—	—	—
se sw 2 17 49	qm	10	—	—	—	—	—	—	—	—	—	—	—	—
se sw 2 18 49	qm	16	—	—	—	—	—	—	—	—	—	—	—	—
sw sw 2 18 49	qm	50	—	—	—	—	—	—	—	—	—	—	—	—
sw ne 3 18 50	qm	2	—	—	—	—	—	—	—	—	—	—	—	—

APPENDIX B

CAPTURE ZONE DELINEATION TABLE

Table B-1. Calculated capture zone widths and thicknesses. Screen elevation based on 1,000-m-thick aquifer.

ID	Screen Elevation (m)	Pump Rate (m ³ /d)	Gradient	Transmissivity (m ² /d)	Width (m)	Thickness (m)	Not Captured on Top (m)
1	940-1,000	1	0.005	100	29	73	—
2	940-1,000	2	0.005	100	54	82	—
3	940-1,000	3	0.005	100	76	88	—
4	940-1,000	4	0.005	100	97	96	—
5	940-1,000	6.815	0.005	100	146	113	—
6	940-1,000	37.5	0.005	100	418	224	—
7	940-1,000	75	0.005	100	607	309	—
8	940-1,000	300	0.005	100	1292	575	—
9	940-1,000	800	0.005	100	2330	825	—
10	940-1,000	1380	0.005	100	3382	941	—
11	940-1,000	2000	0.005	100	4450	985	—
12	940-1,000	3	0.005	10	369	203	—
13	940-1,000	3	0.005	50	133	108	—
14	940-1,000	3	0.005	100	76	88	—
15	940-1,000	3	0.005	400	22	70	—
16	940-1,000	3	0.001	100	248	151	—
17	940-1,000	3	0.0025	100	133	108	—
18	940-1,000	3	0.005	100	76	88	—
19	940-1,000	3	0.05	100	41	78	—
20	940-1,000	3	0.005	100	76	88	—

B-1

Table B-1. Table of calculated capture zone widths and thicknesses. Screen elevation based on 1,000-m-thick aquifer. (cont'd)

ID	Screen Elevation (m)	Pump Rate (m ³ /d)	Gradient	Transmissivity (m ² /d)	Width (m)	Thickness (m)	Not Captured on Top (m)
21	930-990	3	0.005	100	69	98	0.2
22	920-980	3	0.005	100	67	107	5
23	900-960	3	0.005	100	68	127	21
24	980-1,000	3	0.005	100	115	65	—
25	940-1,000	3	0.005	100	76	88	—
26	900-1,000	3	0.005	100	51	122	—
27	0-1,000	300	0.005	100	574	1000	—
28	500-1,000	300	0.005	100	940	752	—
29	810-1,000	300	0.005	100	1238	601	—
30	940-1,000	300	0.005	100	1292	575	—
31	940-1,000	300	0.005	50	1944	751	—
32	940-1,000	300	0.005	100	1292	575	—
33	940-1,000	300	0.005	200	876	424	—
34	940-1,000	300	0.005	300	705	352	—
35	940-1,000	300	0.005	400	607	309	—
36	940-1,000	2116	0.005	200	2810	890	—
37	940-1,000	2116	0.005	300	2146	793	—
38	940-1,000	2116	0.005	400	1798	719	—
39	940-1,000	2116	0.001	100	5596	1000	—
40	940-1,000	2116	0.002	100	3282	934	—

B-2

Table B-1. Table of calculated capture zone widths and thicknesses. Screen elevation based on 1,000-m-thick aquifer. (cont'd)

ID	Screen Elevation (m)	Pump Rate (m³/d)	Gradient	Transmissivity (m²/d)	Width (m)	Thickness (m)	Not Captured on Top (m)
41	940-1,000	2116	0.003	100	2486	850	—
42	940-1,000	2116	0.005	100	1798	719	—

L

L

L

APPENDIX C

TABLE OF BOREHOLE DILUTION FACTORS

Table C-1. Calculated dilution factors for combinations of plume scenarios and capture zones at 25 km. Capture #ID in column No. 2 are in reference to table in appendix B; Q = pumping rate (m³/d), T = transmissivity (m²/d), grad = regional gradient. The dilution factors are V-BDF (volumetric flux-based borehole dilution factor), P-DF (point dilution factor based on centerline concentration), and T-BDF (dispersion during transport-based borehole dilution factor). Additional significant figures are reported to illustrate relative differences only.

Plume Description	Capture Description	V-BDF	P-DF	T-BDF
3D plume 1				
20:2:0.2 m	#8, Q = 300	1.4	9.1	34
20:2:0.2 m	#9, Q = 800	2.6	9.1	55
20:2:0.2 m	#10, Q = 1,380	3.5	9.1	57
20:2:0.2 m	#11, Q = 2,000	4.8	9.1	57
Small irrigation well, 3D plume 1				
20:2:0.2 m	#31, T = 50	2.6	9.1	48
20:2:0.2 m	#32, T = 100	1.8	9.1	34
20:2:0.2 m	#33, T = 200	1.4	9.1	26
20:2:0.2 m	#34, T = 300	1.0	9.1	20
20:2:0.2 m	#35, T = 400	1.0	9.1	18
Large irrigation well, 3D plume 1				
20:2:0.2 m	#36, T = 200	2.8	9.1	57
20:2:0.2 m	#37, T = 300	3.0	9.1	52
20:2:0.2 m	#38, T = 400	2.4	9.1	45
20:2:0.2 m	#39, grad = 0.001	6.2	9.1	57.5
20:2:0.2 m	#40, grad = 0.002	3.4	9.1	57.5
20:2:0.2 m	#41, grad = 0.003	2.3	9.1	56.6
20:2:0.2 m	#42, grad = 0.005	1.0	9.1	45
Domestic wells, 3D plume 1				
20:2:0.2m	#21, 940-1,000	9.1	9.5	1
20:2:0.2 m	#22, 930-990	9.1	9.7	1
20:2:0.2 m	#23, 920-980	9.1	9.9	1
20:2:0.2 m	#24, 900-960	9.1	10.4	1
20:2:0.2 m	#1, Q = 1	9.1	9.36	1

Table C-1. Calculated dilution factors for combinations of plume scenarios and capture zones at 25 km. Capture #ID in column No. 2 are in reference to table in appendix B; Q = pumping rate (m³/d), T = transmissivity (m²/d), grad = regional gradient. The dilution factors are V-BDF (volumetric flux-based borehole dilution factor), P-DF (point dilution factor based on centerline concentration), and T-BDF (dispersion during transport-based borehole dilution factor). Additional significant figures are reported to illustrate relative differences only. (cont'd)

Plume Description	Capture Description	V-BDF	P-DF	T-BDF
20:2:0.2 m	#2, Q = 2	9.1	9.44	1
20:2:0.2 m	#3, Q = 3	9.1	9.5	1
20:2:0.2 m	#4, Q = 4	9.1	9.6	1
20:2:0.2 m	#5, Q = 6.8	9.1	9.9	1
20:2:0.2 m	#6, Q = 37.5	9.1	13	1
20:2:0.2 m	#7, Q = 75	9.1	18	1
20:2:0.2 m	#12, T = 10	9.1	12	1
20:2:0.2 m	#13, T = 50	9.1	9.8	1
20:2:0.2 m	#14, T = 100	9.1	9.5	1
20:2:0.2 m	#15, T = 400	9.1	9.3	1
20:2:0.2 m	#16, grad = 0.001	9.1	11	1
20:2:0.2 m	#17, grad = 0.0025	9.1	9.8	1
20:2:0.2 m	#18, grad = 0.005	9.1	9.5	1
20:2:0.2 m	#19, grad = 0.01	9.1	9.4	1
3D plume 2				
100:10:0.1 m	#8, Q = 300	1.9	14	37
100:10:0.1 m	#9, Q = 800	2.7	14	47
100:10:0.1 m	#10, Q = 1,380	3.3	14	60
100:10:0.1 m	#11, Q = 2,000	4.1	14	73
Small irrigation well, 3D plume 2				
100:10:0.1 m	#31, T = 50	3.2	14	43
100:10:0.1 m	#32, T = 100	2.4	14	37
100:10:0.1 m	#33, T = 200	1.8	14	34
100:10:0.1 m	#34, T = 300	1.6	14	32
100:10:0.1 m	#35, T = 400	1.5	14	30

Table C-1. Calculated dilution factors for combinations of plume scenarios and capture zones at 25 km. Capture #ID in column No. 2 are in reference to table in appendix B; Q = pumping rate (m³/d), T = transmissivity (m²/d), grad = regional gradient. The dilution factors are V-BDF (volumetric flux-based borehole dilution factor), P-DF (point dilution factor based on centerline concentration), and T-BDF (dispersion during transport-based borehole dilution factor). Additional significant figures are reported to illustrate relative differences only. (cont'd)

Plume Description	Capture Description	V-BDF	P-DF	T-BDF
Large irrigation well, plume 2				
100:10:0.1 m	#36, T = 200	3.0	14	53
100:10:0.1 m	#37, T = 300	2.6	14	45
100:10:0.1 m	#38, T = 400	2.3	14	41
100:10:0.1 m	#39, grad = 0.001	4.3	14	—
100:10:0.1 m	#40, grad = 0.002	3.3	14	59
100:10:0.1 m	#41, grad = 0.003	2.8	14	49
100:10:0.1 m	#42, grad = 0.005	2.3	14	41
Thin plumes, Domestic wells at 25 km, 20:2 m dispersivity ratio				
25 m thick; 20:2 m	#21, 940-1,000	3.3	1.8	1.78
25 m thick; 20:2 m	#22, 930-990	4.3	1.8	1.77
25 m thick; 20:2 m	#23, 920-980	5.4	1.8	1.77
25 m thick; 20:2 m	#24, 900-960	43	1.8	1.76
10 m thick; 20:2 m	#21, S = 940-1,000	8.2	1.8	1.78
10 m thick; 20:2 m	#22, S = 930-990	10.3	1.8	1.77
10 m thick; 20:2 m	#23, S = 920-980	26	1.8	1.70
10 m thick; 20:2 m	#24, S = 900-960	N/A	1.8	N/A
25 m thick; 20:2 m	#1, Q = 1	2.8	1.8	1.76
25 m thick; 20:2 m	#2, Q = 2	3.1	1.8	1.77
25 m thick; 20:2 m	#3, Q = 3	3.3	1.8	1.78
25 m thick; 20:2 m	#4, Q = 4	3.5	1.8	1.78
25 m thick; 20:2 m	#5, Q = 6.8	4.0	1.8	1.80
25 m thick; 20:2 m	#6, Q = 37.5	7.6	1.8	1.90
25 m thick; 20:2 m	#7, Q = 75	10.2	1.8	2.01
10 m thick; 20:2 m	#1, Q = 1	7.0	1.8	1.76

Table C-1. Calculated dilution factors for combinations of plume scenarios and capture zones at 25 km. Capture #ID in column No. 2 are in reference to table in appendix B; Q = pumping rate (m³/d), T = transmissivity (m²/d), grad = regional gradient. The dilution factors are V-BDF (volumetric flux-based borehole dilution factor), P-DF (point dilution factor based on centerline concentration), and T-BDF (dispersion during transport-based borehole dilution factor). Additional significant figures are reported to illustrate relative differences only. (cont'd)

Plume Description	Capture Description	V-BDF	P-DF	T-BDF
10 m thick; 20:2 m	#2, Q = 2	7.7	1.8	1.77
10 m thick; 20:2 m	#3, Q = 3	8.2	1.8	1.78
10 m thick; 20:2 m	#4, Q = 4	8.8	1.8	1.78
10 m thick; 20:2 m	#5, Q = 6.8	10.1	1.8	1.80
10 m thick; 20:2 m	#6, Q = 37.5	19	1.8	1.90
10 m thick; 20:2 m	#7, Q = 75	26	1.8	2.01
25 m thick; 20:2 m	#12, T = 10	6.9	1.8	1.88
25 m thick; 20:2 m	#13, T = 50	3.9	1.8	1.80
25 m thick; 20:2 m	#14, T = 100	3.3	1.8	1.78
25 m thick; 20:2 m	#15, T = 400	2.7	1.8	1.76
25 m thick; 20:2 m	#16, grad = 0.001	5.3	1.8	1.84
25 m thick; 20:2 m	#17, grad = 0.0025	3.9	1.8	1.80
25 m thick; 20:2 m	#18, grad = 0.005	3.3	1.8	1.78
25 m thick; 20:2 m	#19, grad = 0.01	2.9	1.8	1.77
10 m thick; 20:2 m	#12, T = 10	17	1.8	1.88
10 m thick; 20:2 m	#13, T = 50	9.8	1.8	1.80
10 m thick; 20:2 m	#14, T = 100	8.2	1.8	1.78
10 m thick; 20:2 m	#15, T = 400	6.8	1.8	1.76
10 m thick; 20:2 m	#16, grad = 0.001	13.2	1.8	1.84
10 m thick; 20:2 m	#17, grad = 0.0025	9.8	1.8	1.80
10 m thick; 20:2 m	#18, grad = 0.005	8.2	1.8	1.78
10 m thick; 20:2 m	#19, grad = 0.01	7.4	1.8	1.77
Thin plumes irrigation wells @ 25 km				
25m thick; 20:2 m	#8, Q = 300	19	1.8	2.8
25m thick; 20:2 m	#9, Q = 800	26	1.8	4.8

Table C-1. Calculated dilution factors for combinations of plume scenarios and capture zones at 25 km. Capture #ID in column No. 2 are in reference to table in appendix B; Q = pumping rate (m³/d), T = transmissivity (m²/d), grad = regional gradient. The dilution factors are V-BDF (volumetric flux-based borehole dilution factor), P-DF (point dilution factor based on centerline concentration), and T-BDF (dispersion during transport-based borehole dilution factor). Additional significant figures are reported to illustrate relative differences only. (cont'd)

Plume Description	Capture Description	V-BDF	P-DF	T-BDF
25m thick; 20:2 m	#10, Q = 1,380	36	1.8	5.9
25m thick; 20:2 m	#11, Q = 2,000	49	1.8	5.9
25m thick; 50:5 m	#8, Q = 300	19	2.6	3.3
25m thick; 50:5 m	#9, Q = 800	26	2.6	4.8
25m thick; 50:5 m	#10, Q = 1,380	30	2.6	6.8
25m thick; 50:5 m	#11, Q = 2,000	33	2.6	8.8
25m thick; 100:10 m	#8, Q = 300	19	3.6	4.1
25m thick; 100:10 m	#9, Q = 800	26	3.6	5.2
25m thick; 100:10 m	#10, Q = 1,380	30	3.6	6.9
25m thick; 100:10 m	#11, Q = 2,000	32	3.6	8.9